

Superconducting electronics and detectors workshop overview

Superconducting electronics and detectors workshop

Alexandre Camsonne

Hall A Jefferson Laboratory

September 28th 2022

Outline

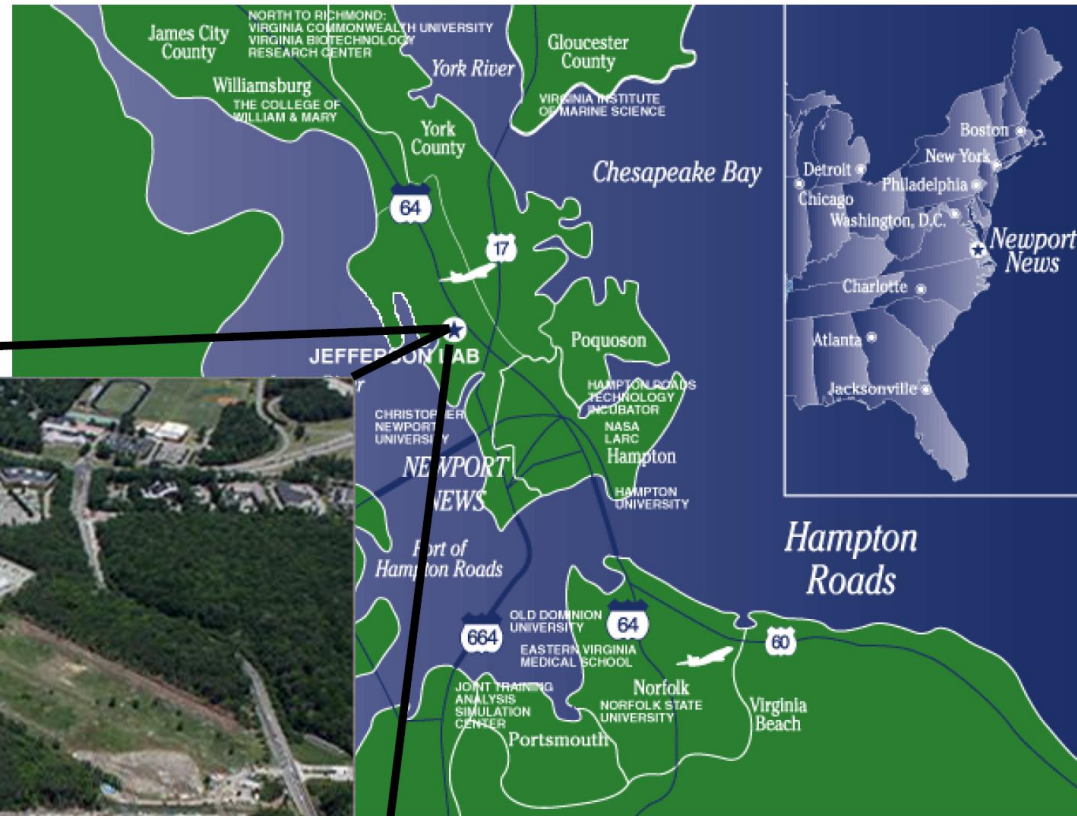
- New developments since 2015
- Experiments and experimental requirements
- Superconducting detector
 - Overview superconducting detectors
 - Superconducting Nanowire technique
 - Properties of superconducting nanowire
- Fabrication
- Superconducting electronics
- Possible applications
- Conclusion

New developments since 2015

- First workshop 2015
 - Focused on SNSPDs
 - Beginning activity at Argonne and JLab
 - C3 program on going
- 2022 workshop
 - Operation of SNSPD in magnetic field
 - C3 completion
 - Quantum computing
 - Broader superconducting detectors for QC and other application and emphasis on readout
 - EIC detectors

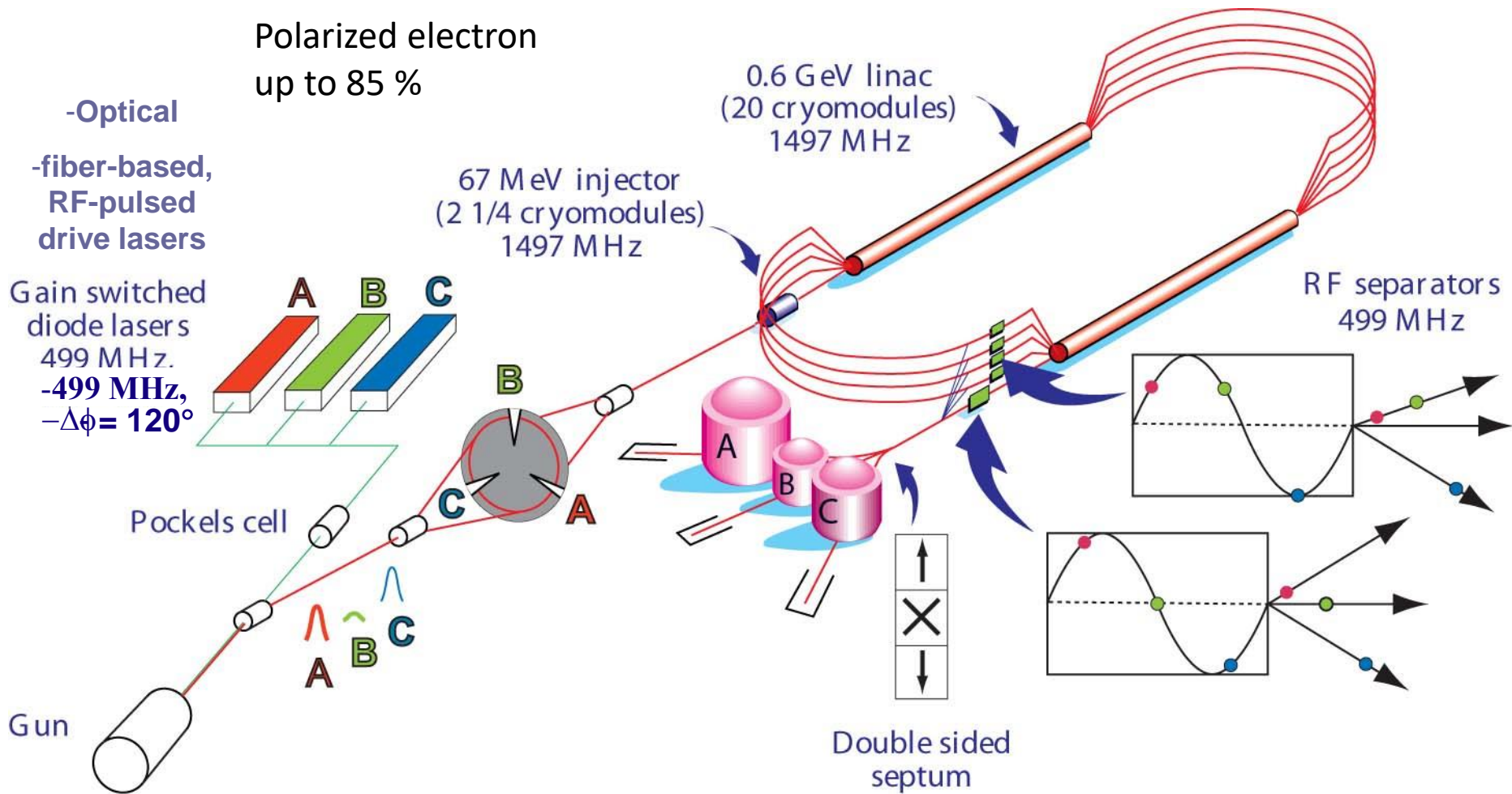
Jefferson Laboratory

Newport News
Virginia
USA

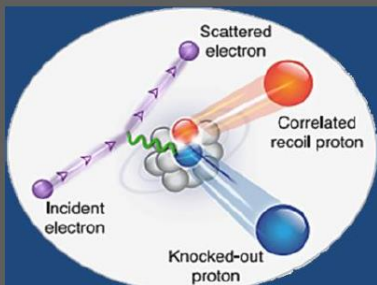


Electron beam accelerator
2 superconducting LINACs
5 ARCs
3 experimental Halls

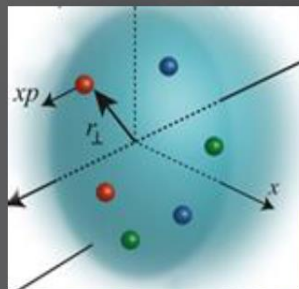
Continuous Electron Beam Accelerator Facility



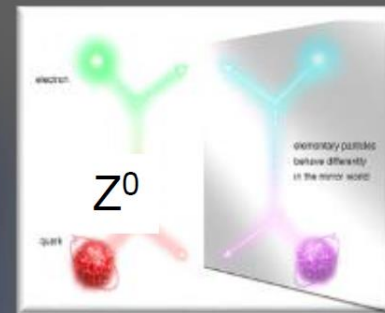
Jefferson Lab: A Laboratory For Nuclear Science



Nuclear Structure



Structure of Hadrons



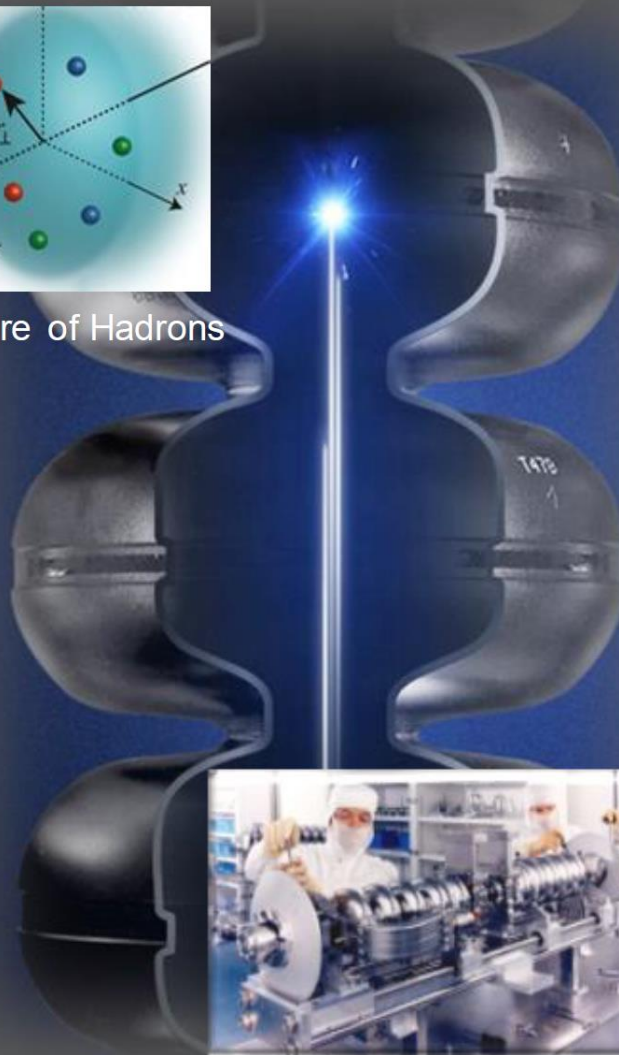
Fundamental Forces & Symmetries



Medical Imaging Technology



Cryogenics



Accelerator S&T



Nuclear Astrophysics



Theory & Computation

CEBAF AT JEFFERSON LAB

Jefferson Lab's Continuous Electron Beam Accelerator Facility (CEBAF) enables world-class fundamental research of the atom's nucleus. Like a giant microscope, it allows scientists to "see" things a million times smaller than an atom.



1 INJECTOR

The injector produces electron beams for experiments.



2 LINEAR ACCELERATOR

The straight portions of CEBAF, the linacs, each have 25 sections of accelerator called cryomodules. Electrons travel up to 5.5 passes through the linacs to reach 12 GeV.



3 CENTRAL HELIUM LIQUEFIER

The Central Helium Liquefier keeps the accelerator cavities at -456 degrees Fahrenheit.



4 RECIRCULATION MAGNETS

Quadrupole and dipole magnets in the tunnel focus and steer the beam as it passes through each arc.



5 EXPERIMENTAL HALL A

Hall A is configured with two High Resolution Spectrometers for precise measurements of the inner structure of nuclei. The hall is also used for one-of-a-kind, large-installation experiments.



6 EXPERIMENTAL HALL B

The CEBAF Large Acceptance Spectrometer surrounds the target, permitting researchers to measure simultaneously many different reactions over a broad range of angles.



7 EXPERIMENTAL HALL C

The Super High Momentum Spectrometer and the High Momentum Spectrometer make precise measurements of the inner structure of protons and nuclei at high beam energy and current.



8 EXPERIMENTAL HALL D

Hall D is configured with a superconducting solenoid magnet and associated detector systems that are used to study the strong force that binds quarks together.

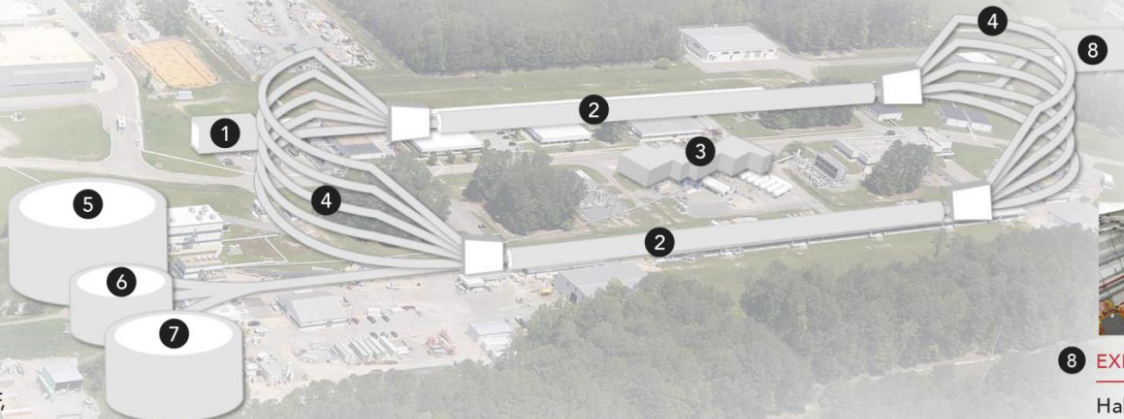
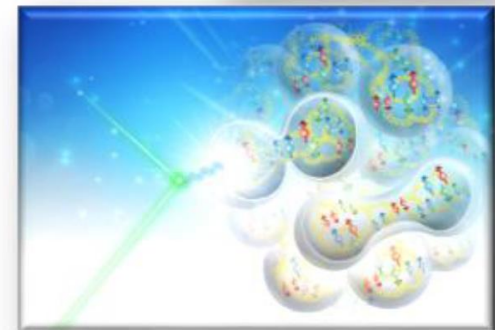
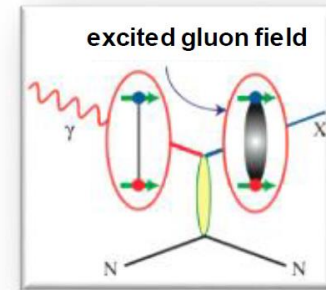


Diagram representational of below ground structure

Jefferson Lab @ 12 GeV Science Questions

- What is the role of gluonic excitations in the spectroscopy of light mesons?
- Where is the missing spin in the nucleon? Role of orbital angular momentum?
- Can we reveal a novel landscape of nucleon substructure through 3D imaging at the femtometer scale?
- What is the relation between short-range N-N correlations, the partonic structure of nuclei, and the nature of the nuclear force?
- Can we discover evidence for physics beyond the standard model of particle physics?

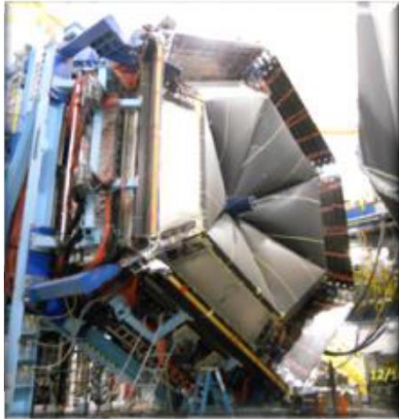


12 GeV Scientific Capabilities

Hall D – exploring origin of **confinement** by studying **exotic mesons**



Hall B – **nucleon imaging** (“femtography”) via **generalized parton distributions** and **transverse momentum distributions**



Hall C – precision determination of **valence quark** properties in nucleons and nuclei



Hall A – short range correlations, form factors, hyper-nuclear physics, **future new experiments (e.g., SoLID and MOLLER)**

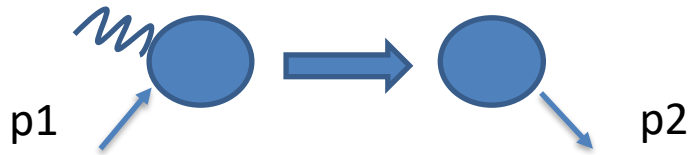


Jefferson Laboratory

- Superconducting accelerator
 - 1499 MHz bunch continuous wave
 - 2.2 to 11 GeV in Hall A,B,C
 - Up to 80 μA
- Cryogenic target
 - 15 cm to 1 m target
- Maximum luminosity around $10^{39} \text{ cm}^{-2}\text{s}^{-1}$
(LHC $5 \times 10^{34} \text{ cm}^{-2}\text{s}^{-1}$)

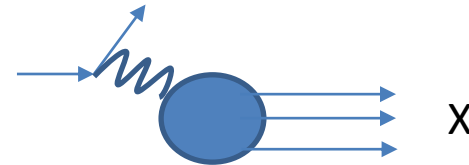
Nucleon structure

- Elastic scattering



- Form factor
- Give spatial distribution of the charge of nucleon but no information on nucleon content

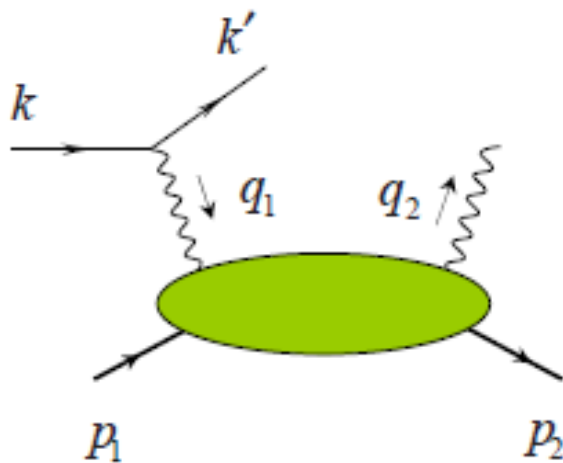
- Deep Inelastic Scattering



- Parton distributions
- Give the content of the nucleon and longitudinal momentum distribution but no transverse information

Generalized Parton Distributions

- New formalism generalizing the concept of form factor and parton distribution
- Non diagonal terms of Compton Scattering
- Accessible by measuring exclusive reactions

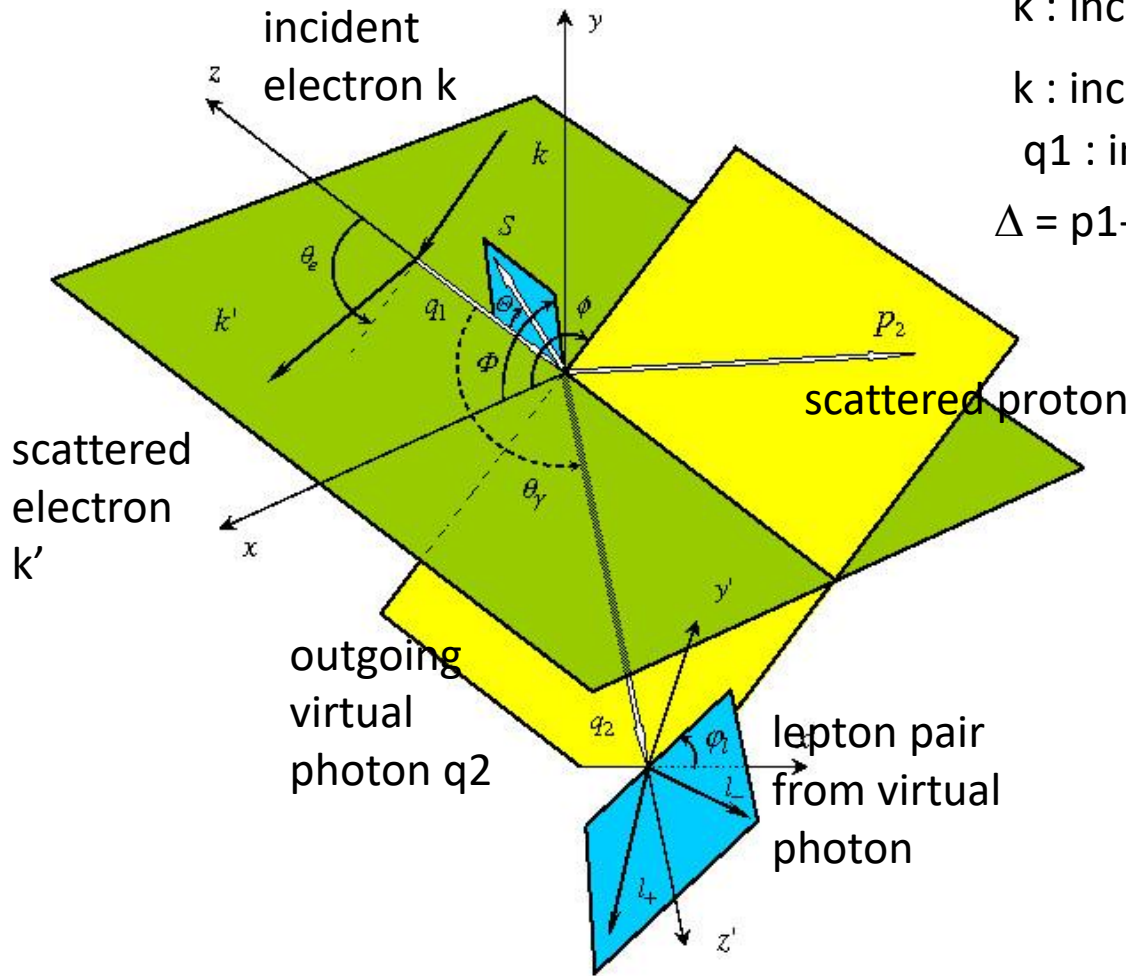


Deeply Virtual Compton Scattering

$$ep \longrightarrow ep\gamma$$

Compton scattering on quarks
inside of the protons

DVCS kinematical variables



k : incident electron of energy E

k : incident electron of energy E'

q_1 : incident virtual photon

$$\Delta = p_1 - p_2 = q_2 - q_1$$

$$Q^2 = -q^2$$

$$p = p_1 + p_2$$

$$q = \frac{1}{2}(q_1 + q_2)$$

$$\xi = \frac{Q^2}{2p \cdot q}$$

$$\eta = \frac{\Delta \cdot q}{p \cdot q}$$

$$Q^2 = -(k - k')^2$$

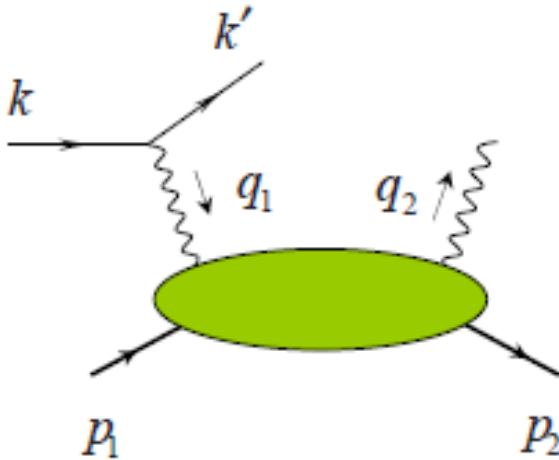
$$x_{bj} = \frac{Q^2}{2p_1 \cdot q_1}$$

Belitsky Radyushkin : Unraveling hadron structure with generalized parton distributions (arXiv:hep-ph/0504030v3 27 Jun 2005)

Generalized parton distributions

$$T_{\mu\nu} = i \int d^4z e^{i(q \cdot z)} \left\langle N(p_1, s_1) | T \left\{ J^\mu \left(-\frac{z}{2} \right), J^\nu \left(\frac{z}{2} \right) \right\} | N(p_1, s_1) \right\rangle$$

$$T_{\mu\nu} = i \int d^4z e^{i(q \cdot z)} \left\langle N(p_1, s_1) | T \left\{ J^\mu \left(-\frac{z}{2} \right), J^\nu \left(\frac{z}{2} \right) \right\} | N(p_2, s_2) \right\rangle$$



$$\Delta = p_1 - p_2 = q_2 - q_1$$

$$p = p_1 + p_2$$

$$Q^2 = -q^2$$

$$q = \frac{1}{2} (q_1 + q_2)$$

$$\eta = \frac{\Delta \cdot q}{p \cdot q}$$

$$Q^2 = -(k - k')^2$$

$$\xi = \frac{Q^2}{2p \cdot q}$$

$$x_{bj} = \frac{Q^2}{2p_1 \cdot q_1}$$

$$\langle p_2 | \mathcal{O}^{qg}(-z^-, z^-) | p_1 \rangle = \int_{-1}^1 dx e^{-izp^+ z^-} \left\{ h^+ H^q(x, \eta, \Delta^2) + e^+ E^q(x, \eta, \Delta^2) \right\},$$

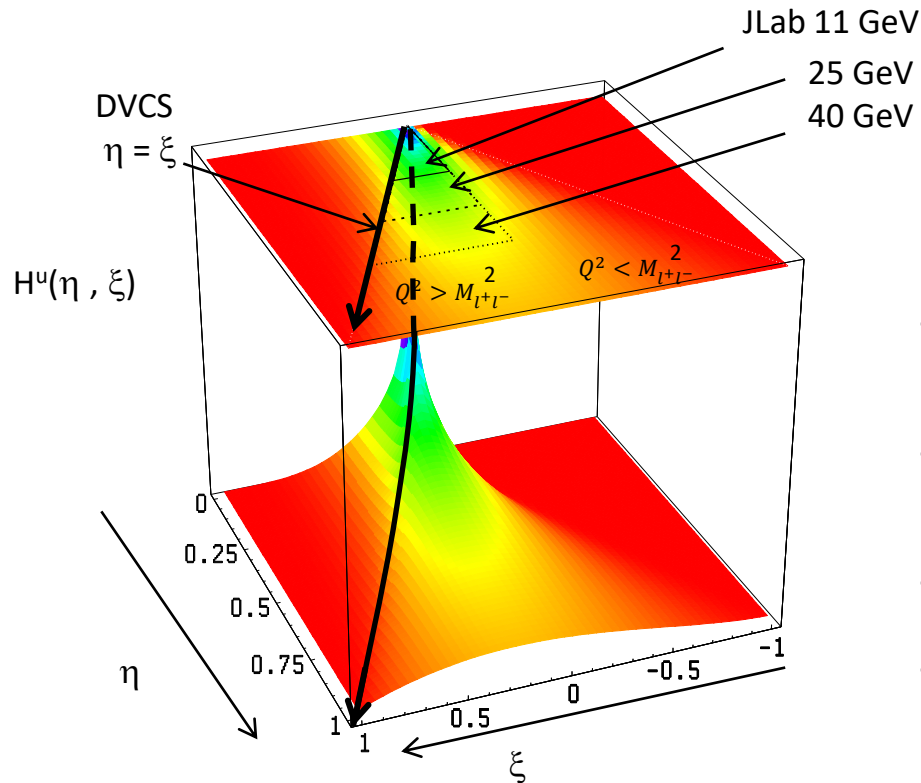
$$\langle p_2 | \tilde{\mathcal{O}}^{qg}(-z^-, z^-) | p_1 \rangle = \int_{-1}^1 dx e^{-izp^+ z^-} \left\{ \tilde{h}^+ \tilde{H}^q(x, \eta, \Delta^2) + \tilde{e}^+ \tilde{E}^q(x, \eta, \Delta^2) \right\},$$

$$\begin{aligned} \langle p_2 | T_\mu^{qg}(-z^-, z^-) | p_1 \rangle = & \int_{-1}^1 dx e^{-izp^+ z^-} \left\{ t^{\frac{1}{2}} H_T^q(x, \eta, \Delta^2) + \frac{p^+ \epsilon_\mu^\perp}{M_N} \tilde{H}_T^q(x, \eta, \Delta^2) \right. \\ & \left. - \frac{1}{2M_N} (\Delta_\mu^\perp h^+ - \Delta^+ h_\mu^\perp) E_T^q(x, \eta, \Delta^2) - \frac{p^+ h_\mu^\perp}{2M_N} \tilde{E}_T^q(x, \eta, \Delta^2) \right\}. \end{aligned}$$

Unraveling nucleon structure with generalized parton distributions Belitsky, Radysuhkin

Arxiv:0504030

GPD model



- DVCS only probes $\eta = \xi$ line
- Example with model of GPD H for up quark
- Jlab : $Q^2 > 0$
- Kinematical range increases with beam energy (larger dilepton mass)

Properties of GPDs

- Forward limit $p_1 = p_1$ $\Delta = 0$ and $\eta = 0$

$$H(x, 0, 0) = f^q(x) \qquad \tilde{H}(x, 0, 0) = \Delta f^q(x)$$

- First moment

$$\int_{-1}^1 dx H^q(x, \eta, \Delta^2) = F_1^q(\Delta^2), \qquad \int_{-1}^1 dx E^q(x, \eta, \Delta^2) = F_2^q(\Delta^2),$$
$$\int_{-1}^1 dx \tilde{H}^q(x, \eta, \Delta^2) = G_A^q(\Delta^2), \qquad \int_{-1}^1 dx \tilde{E}^q(x, \eta, \Delta^2) = G_P^q(\Delta^2)$$

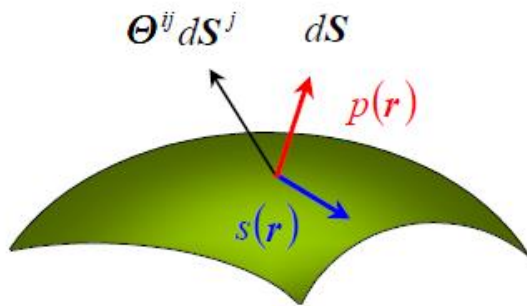
give back the form factors

Proton properties

By integrating GPDs over different variables can access :

- pressure at nucleon surface

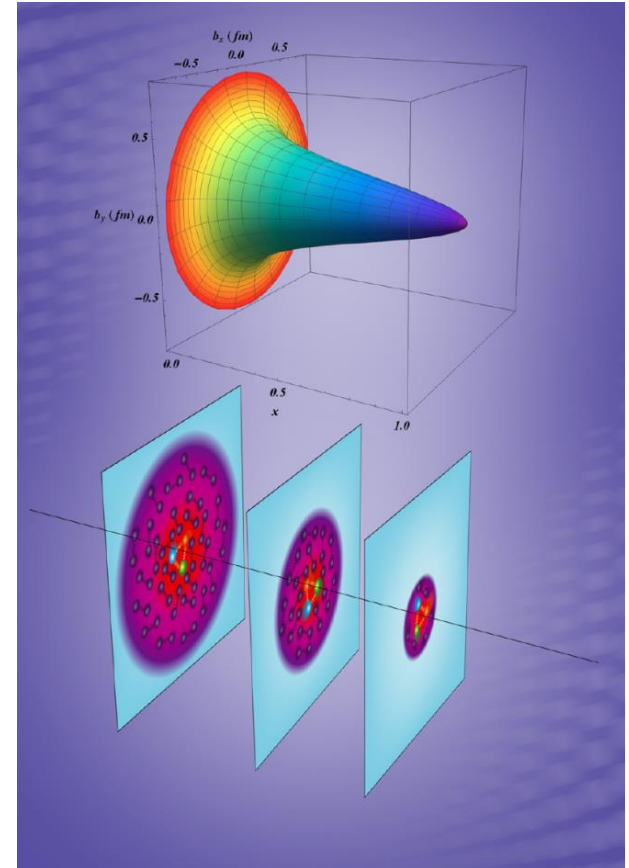
Belitsky Radyushkin : Unraveling hadron structure with generalized parton distributions (arXiv:hep-ph/0504030v3 27 Jun 2005)



[Analysis of Deeply Virtual Compton Scattering Data at Jefferson Lab and Proton Tomography](#)

R. Dupr'e 1, M. Guidal 1, S. Niccolai 1, and M. Vanderhaeghen 2

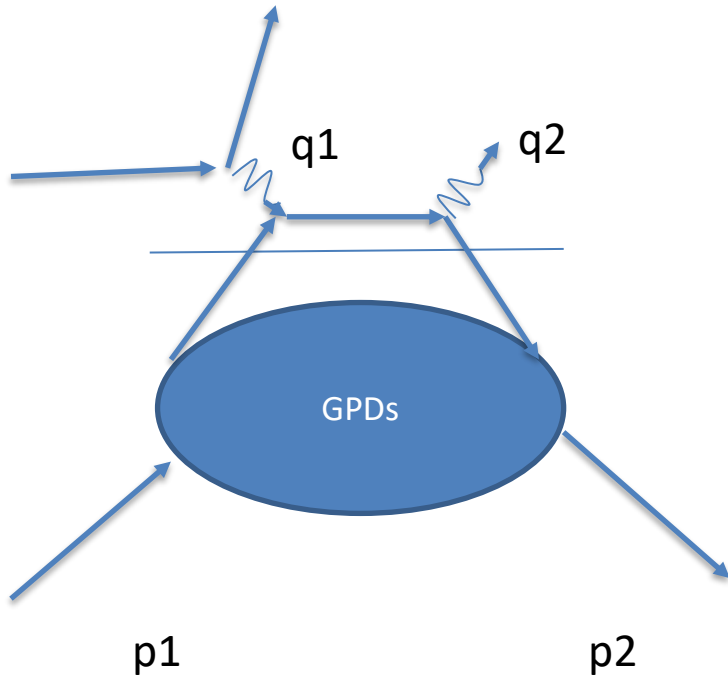
[arXiv:1704.07330](#)



Ji sum rule (access to quark orbital momentum)

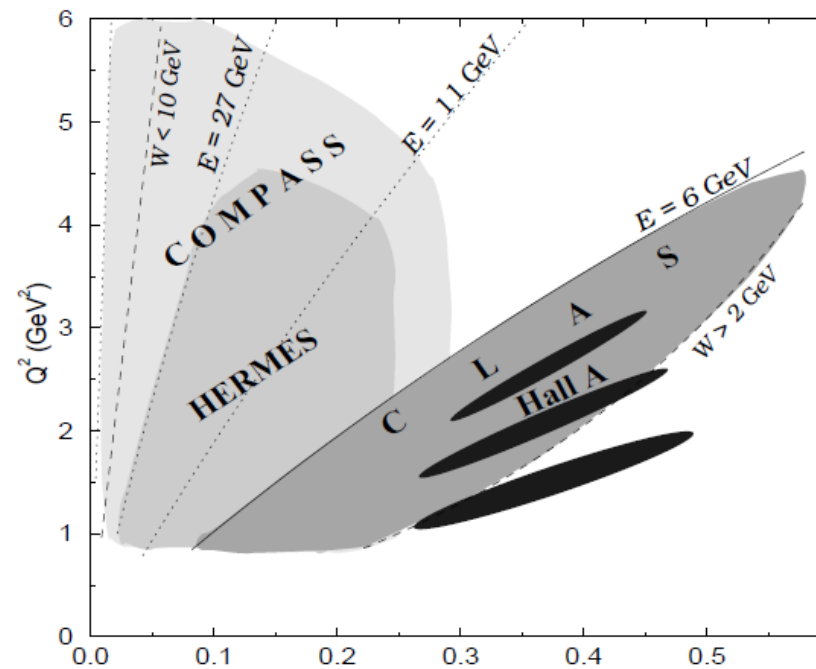
$$\int_{-1}^1 dx x \{H^q(x, \eta, 0) + E^q(x, \eta, 0)\} = 2J^q$$

Deeply Virtual Compton Scattering



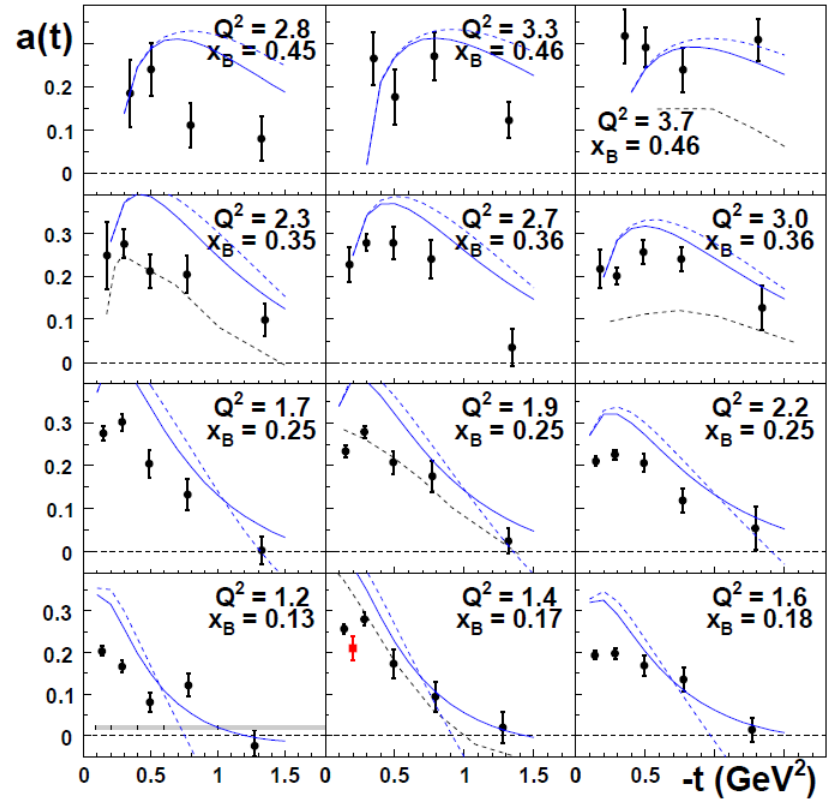
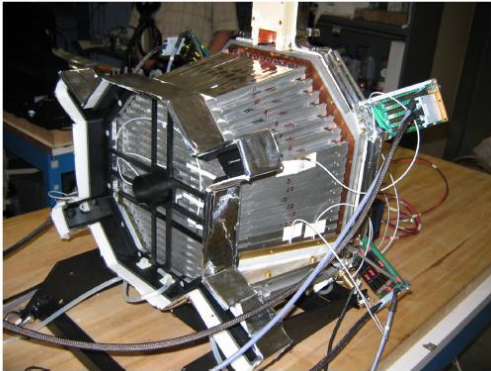
- Handbag diagram
- Factorization theorem need large Q^2 , large s and small t
- Cross-section is product of hard scattering on quark computable with pQCD and the soft non perturbative GPD

Deeply Virtual Compton Scattering at 6 GeV at Jefferson Laboratory

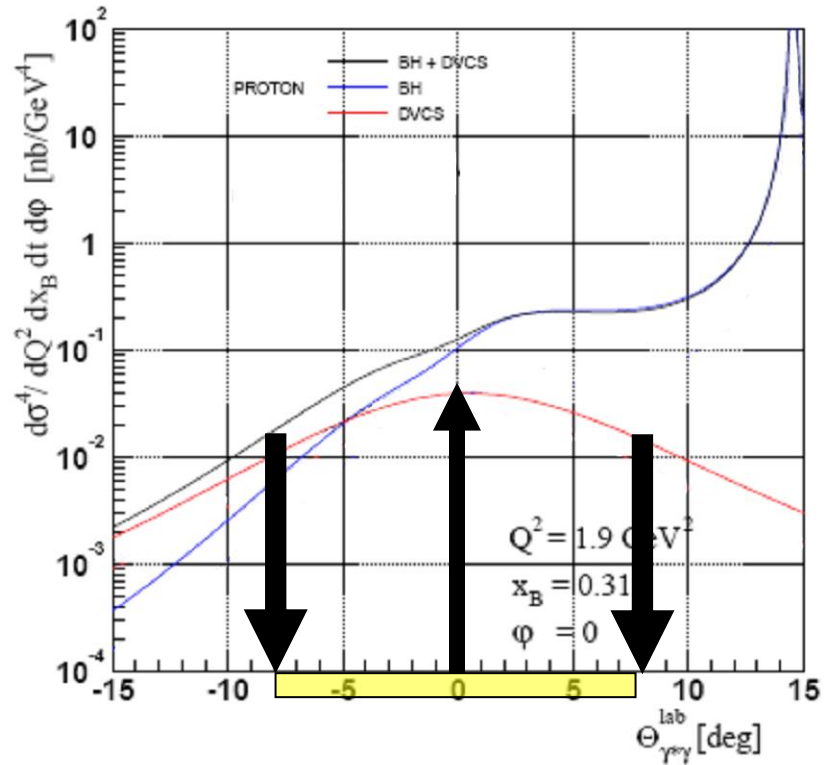
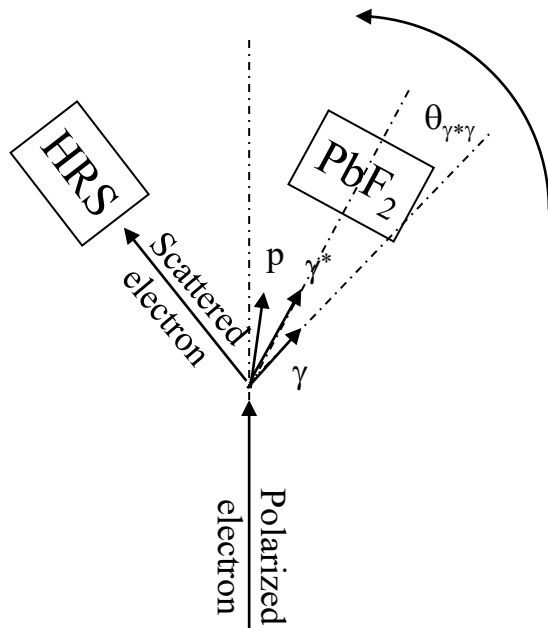


Large acceptance measurement Hall B

$$A = \frac{N^+ - N^-}{N^+ + N^-}$$



Hall A DVCS experiment



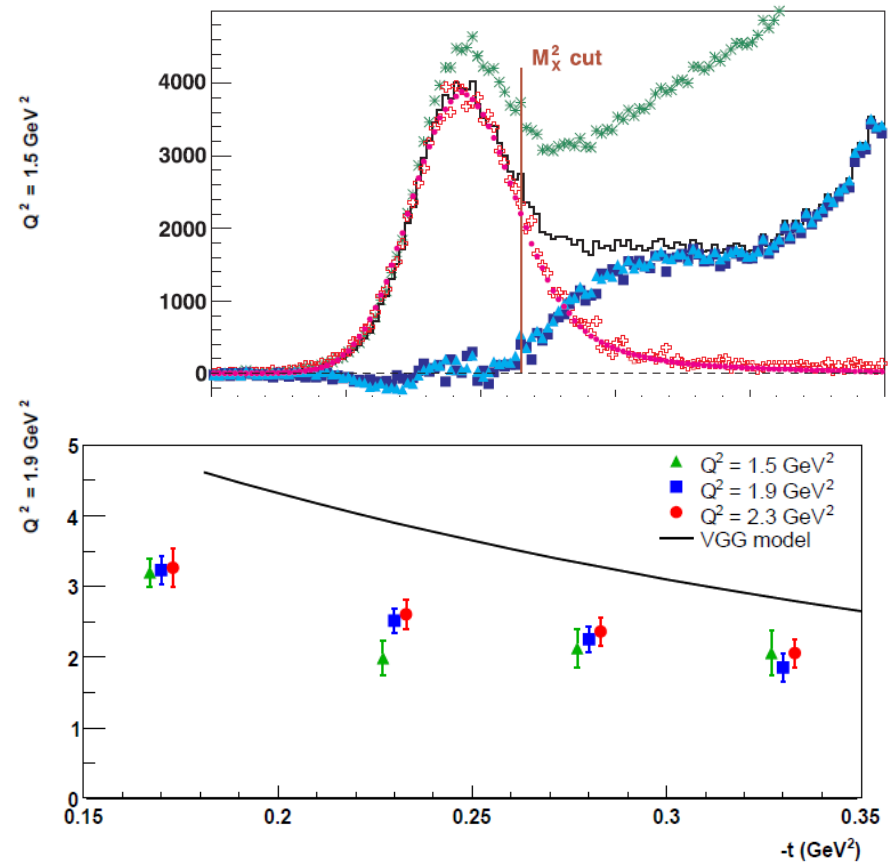
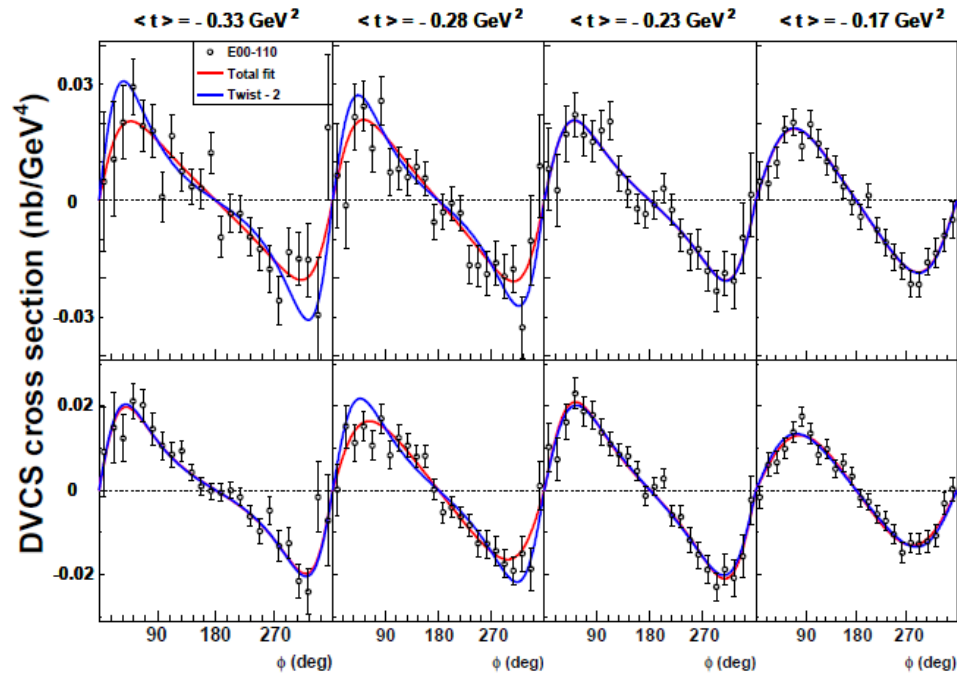
Cross sections measurement

Electron helicity dependent cross sections of photon electroproduction using Jefferson Laboratory polarized electron beam

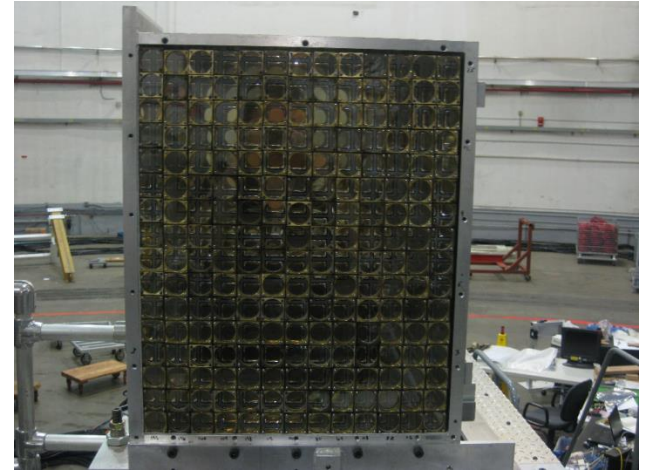
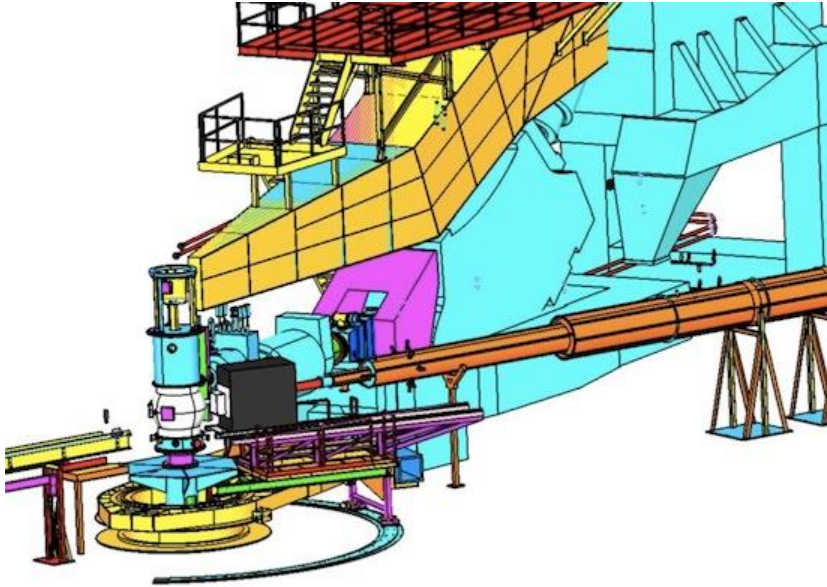
$$d^5 \vec{\sigma} - d^5 \overleftarrow{\sigma} \propto BH \cdot \text{Im}(DVCS) + (\overrightarrow{DVCS}^2 - \overleftarrow{DVCS}^2)$$

$$d^5 \vec{\sigma} + d^5 \overleftarrow{\sigma} \propto BH^2 + \text{Re}(BH \cdot DVCS) + DVCS^2$$

Hall A measurement



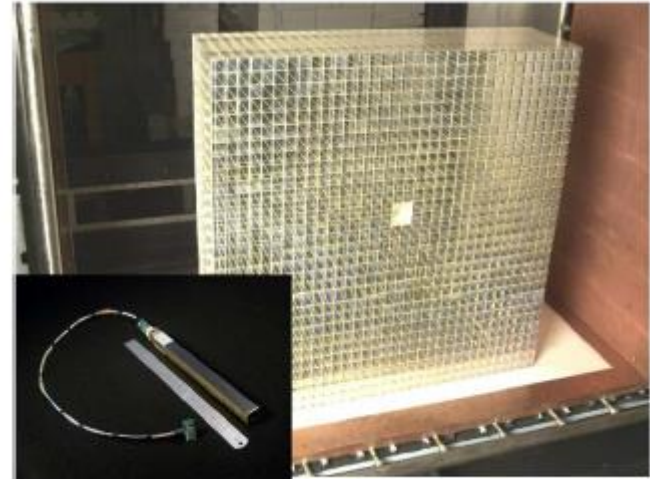
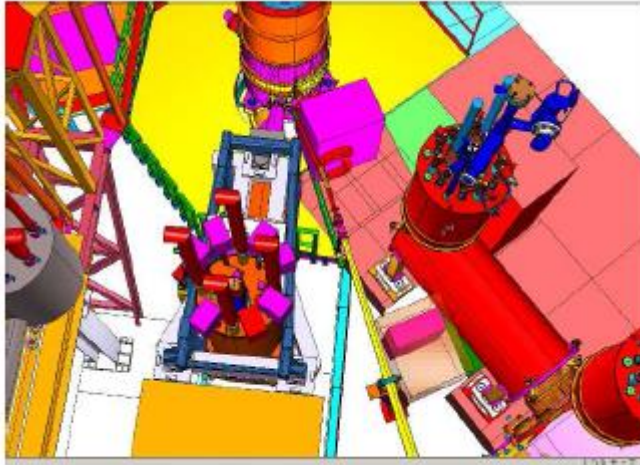
Hall A setup



enlarged calorimeter from 132 to 208 blocks

- 6 GeV experiment completed in 2010
 - [arXiv:1703.09442](https://arxiv.org/abs/1703.09442) Defurne et al.
 - **Phys.Rev.Lett. 117 (2016) no.26, 262001** Defurne et al
- 12 GeV experiment completed end of 2016

Hall C measurement using Neutral Photon Spectrometer



Use Hall C HMS spectrometer with calorimeter carried on new SHMS spectrometer

Use a sweeping magnet and a $^{1116}\text{PbWO}_4$ calorimeter for improved energy resolution

Hall A/C coverage

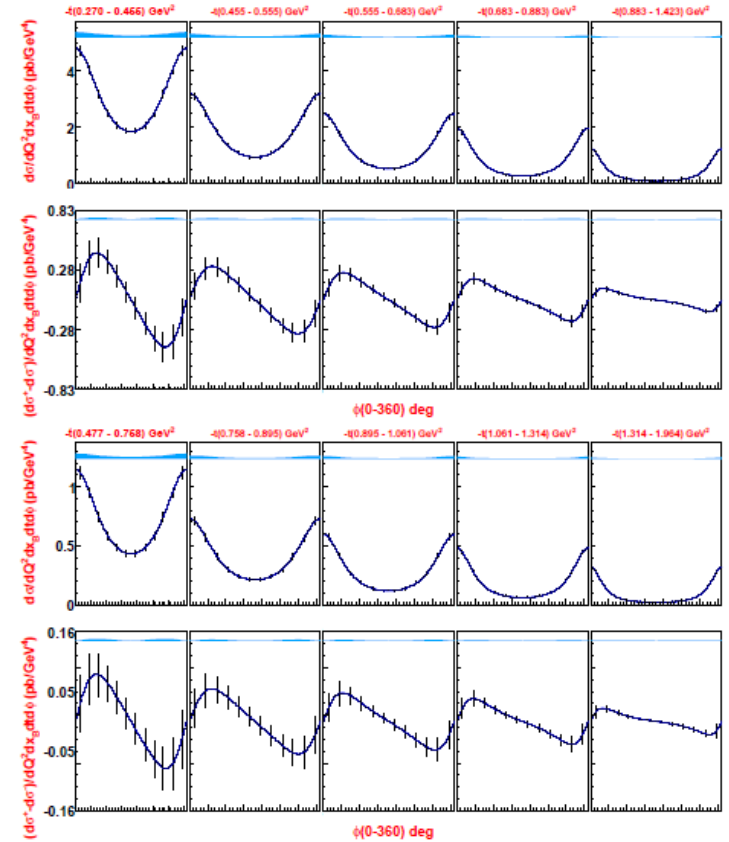
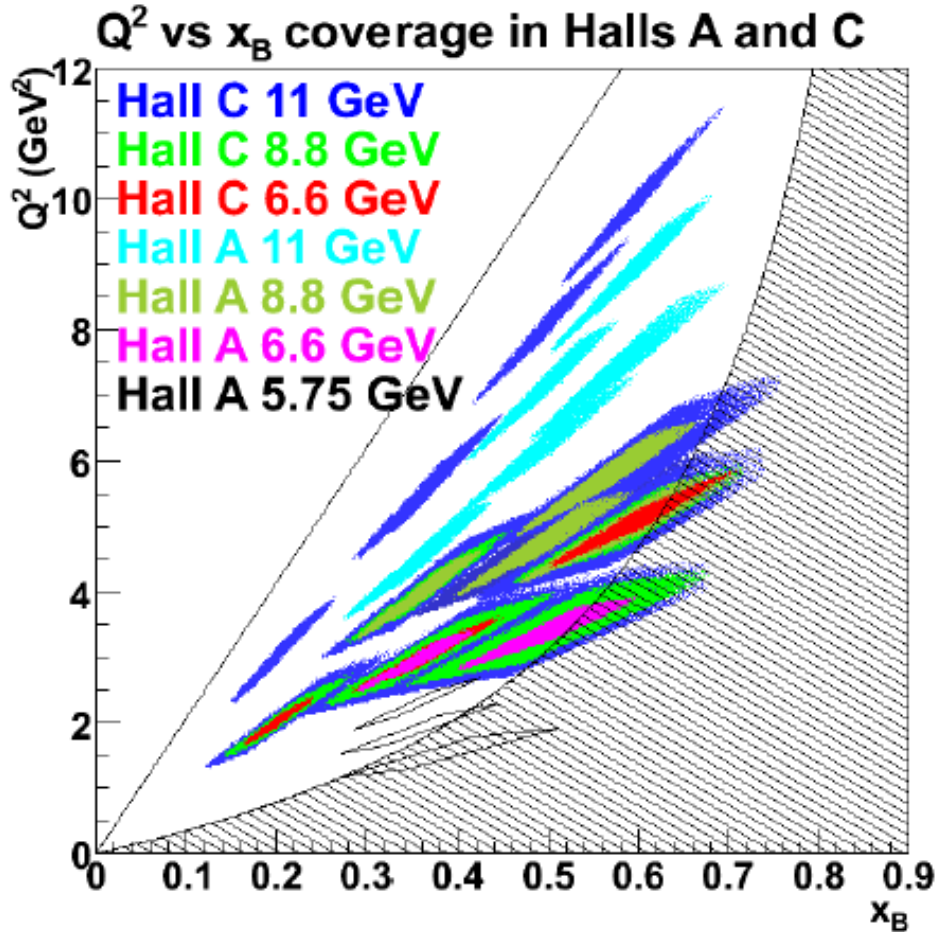
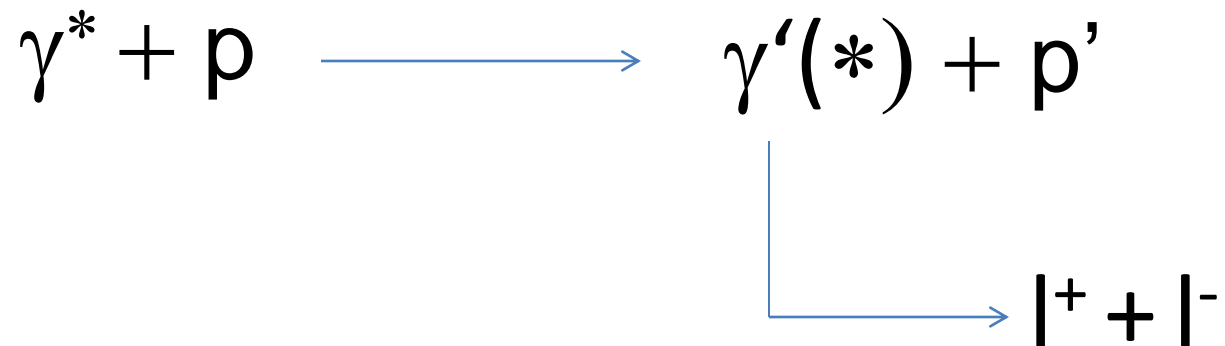


FIG. 12: Projections for the highest Q^2 settings: $Q^2 = 8 \text{ GeV}^2$ (top, $x_B = 0.5$) and $Q^2 = 10 \text{ GeV}^2$ (bottom, $x_B = 0.6$).

DVCS / Double DVCS

$$\gamma^* + p \longrightarrow \gamma'(*) + p'$$


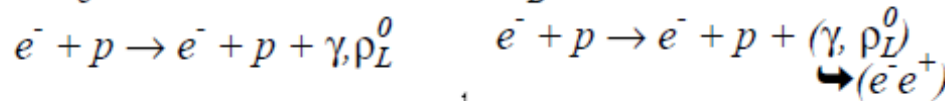
The diagram illustrates the process of Double DVCS. It starts with a virtual photon (γ^*) and a proton (p) on the left. A blue arrow points to the right, leading to a real photon ($\gamma'(*)$) and a proton (p'). From the real photon, a blue L-shaped arrow points down and then right to a lepton pair ($l^+ + l^-$).

Guidal and Vanderhaegen : Double deeply virtual Compton scattering off the nucleon (arXiv:hep-ph/0208275v1 30 Aug 2002)

Belitsky Radyushkin : Unraveling hadron structure with generalized parton distributions (arXiv:hep-ph/0504030v3 27 Jun 2005)

DDVCS cross section

$$E_e = 6 \text{ GeV}, Q^2 = 2.5 \text{ GeV}^2, x_B = 0.3, \Phi = 0 \text{ deg.}$$



- VGG model

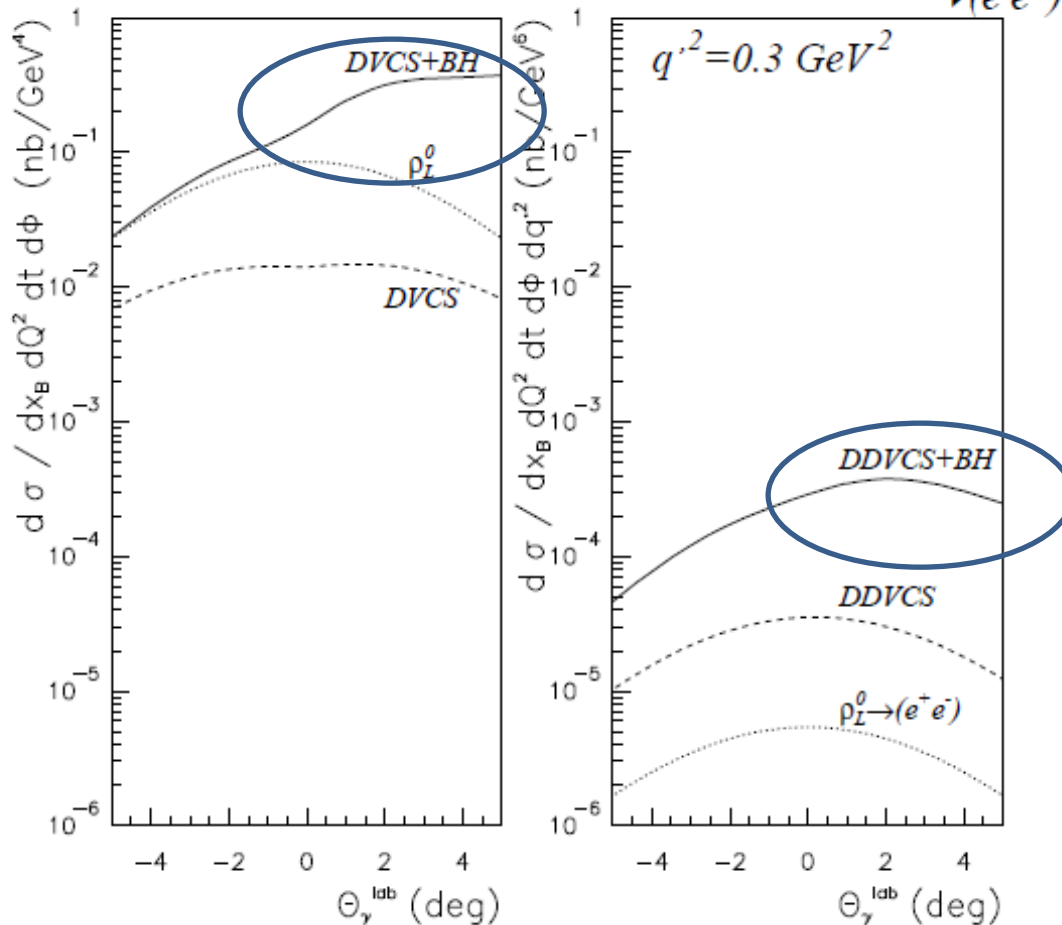
- Order of $\sim 0.1 \text{ pb} = 10^{-36} \text{ cm}^2$

- About 100 smaller than DVCS

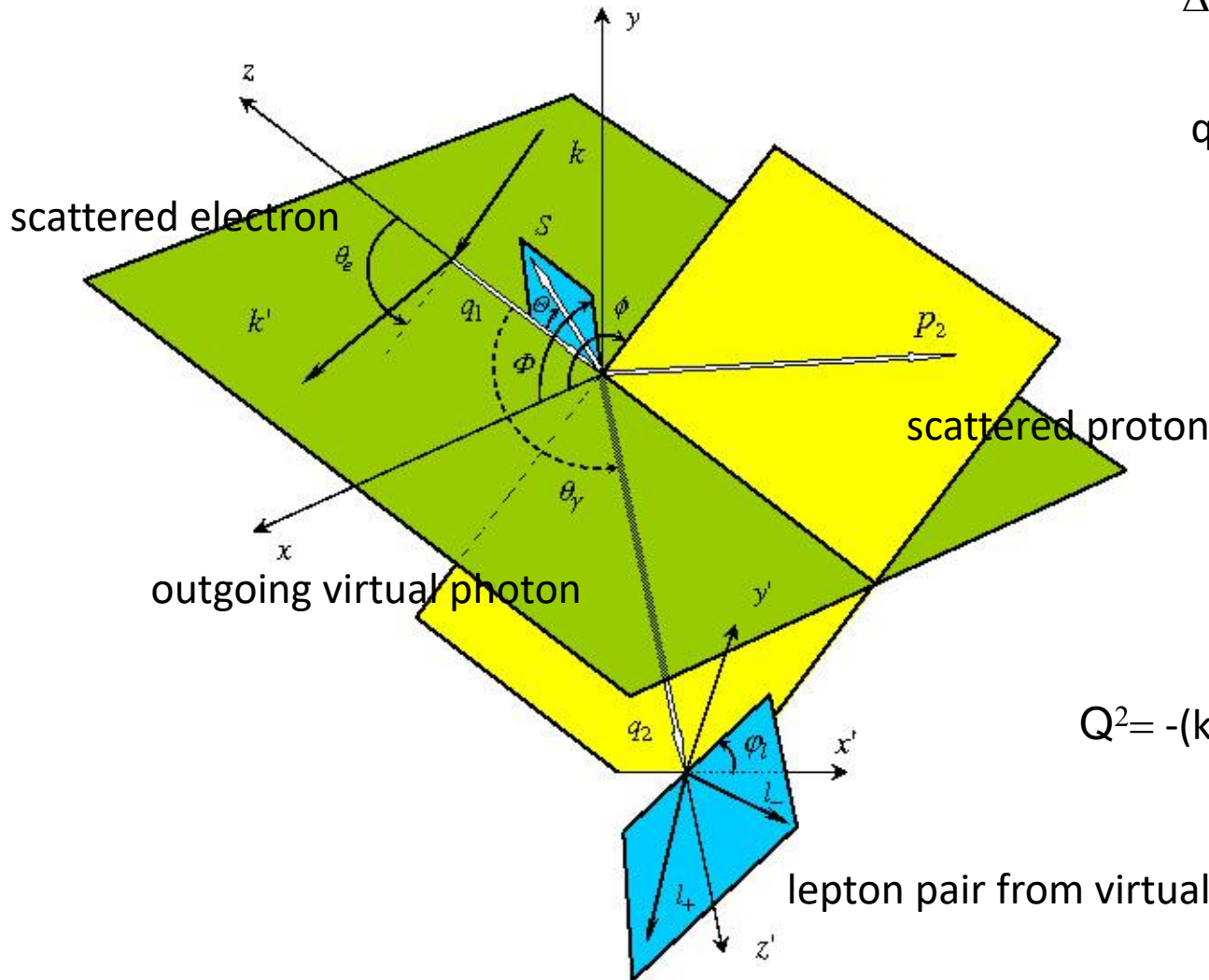
- Virtual Beth and Heitler

- Interference term enhanced by BH

- Contributions from mesons small when far from meson mass



Double Deeply Virtual Compton Scattering



$$\Delta = p_1 - p_2 = q_2 - q_1$$

$$p = p_1 + p_2$$

$$q = \frac{1}{2} (q_1 + q_2)$$

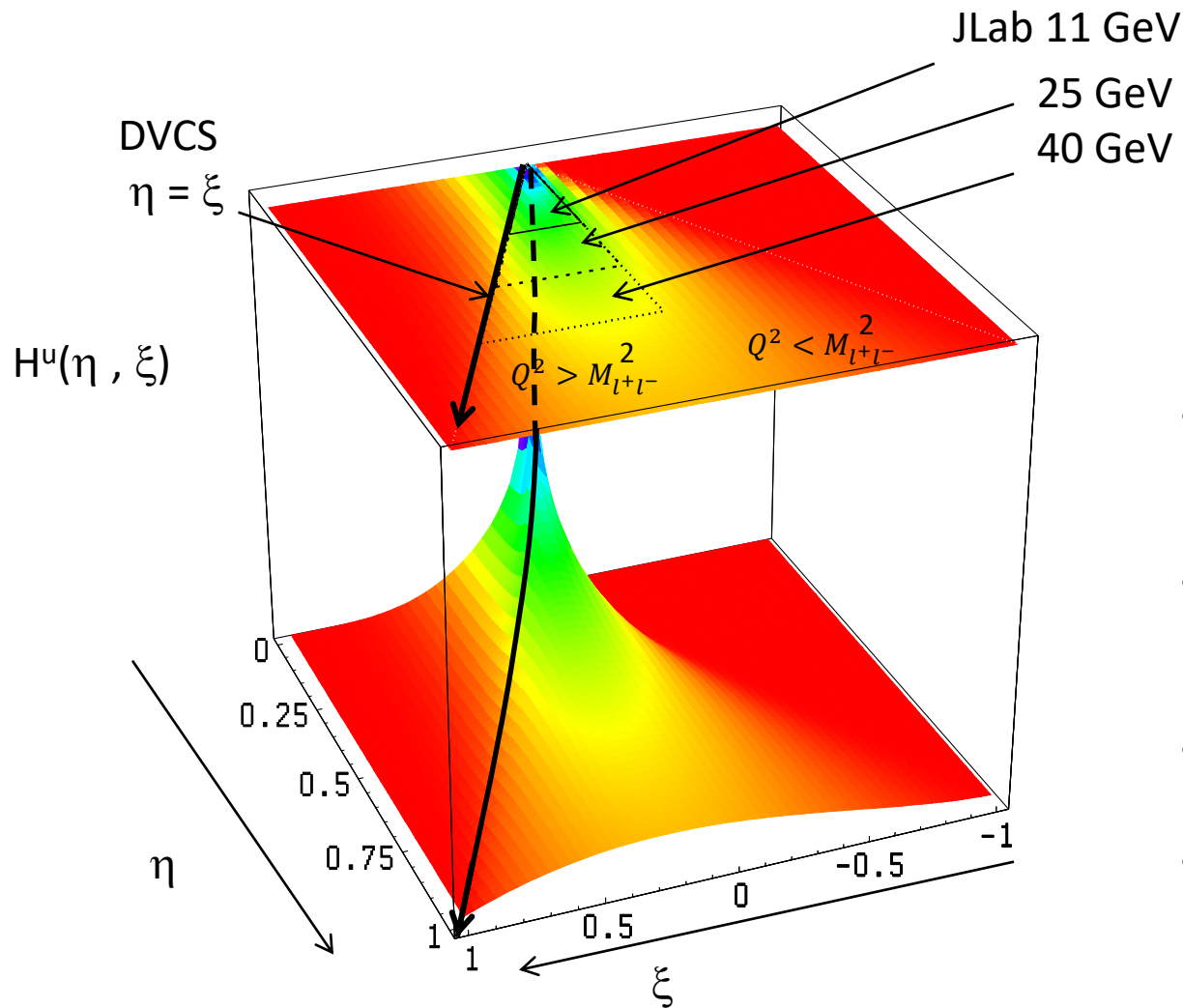
$$Q^2 = -q^2$$

$$\xi = \frac{Q^2}{2p \cdot q}$$

$$\eta = \frac{\Delta \cdot q}{p \cdot q}$$

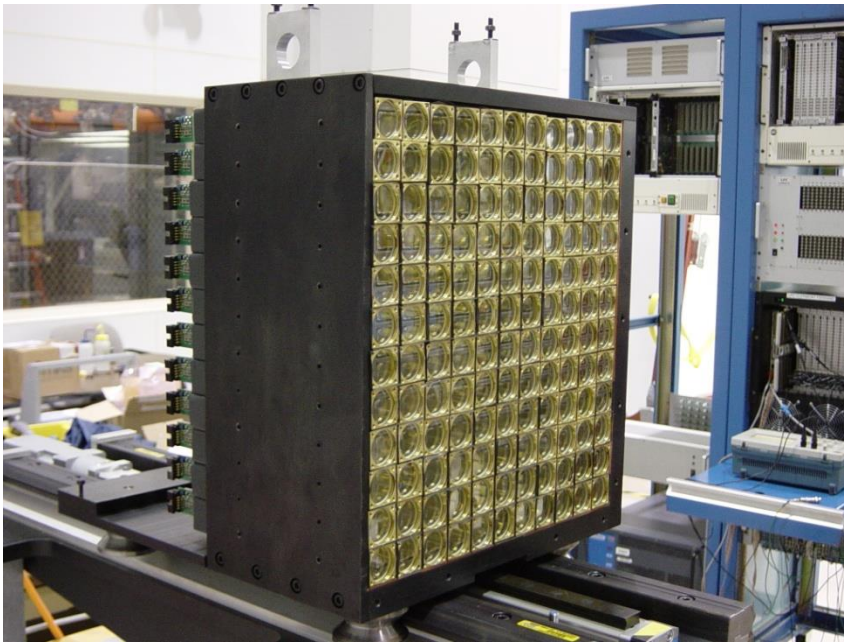
$$Q^2 = -(k - k')^2 \quad x_{bj} = \frac{Q^2}{2p_1 \cdot q_1}$$

Kinematical coverage



- DVCS only probes $\eta = \xi$ line
- Example with model of GPD H for up quark
- Jlab : $Q^2 > 0$
- Kinematical range increases with beam energy (larger dilepton mass)

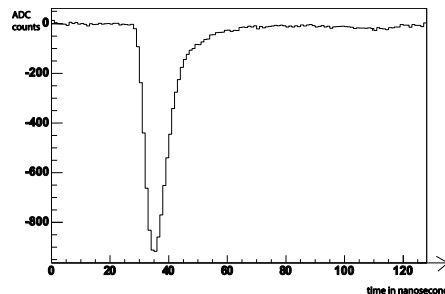
DVCS experiment in Hall A (2005)



11x12 = 132 blocks
3cmx3cmx18.6cm
110 cm from the target
1msr per block

- Lead fluoride
 - Pure Cerenkov : not sensitive to charged hadronic background
 - density 7.77 g.cm³
 - $X_0=0.93$ cm length= $20X_0$
Molière radius = 2.2 cm
 - Good radiation hardness

- PMT R7700 Hamamatsu
 - 8 stages
 - Gain : 10^4
 - Rise time 2 ns
 - FWHM 6 ns

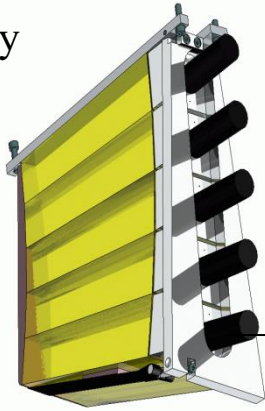


- 1 Photoelectron per MeV,
- Energy resolution 4
.2GeV :
2.4 %
- Position resolution:
2 mm

PMT detector signal

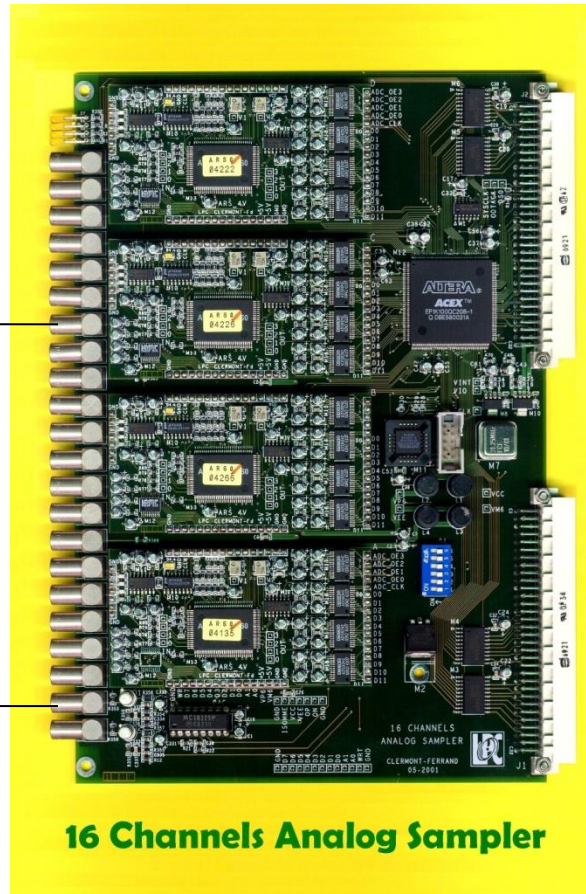
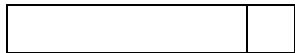
- Sampling system
 - 1GHz Analog Memory sampling system

Proton Array



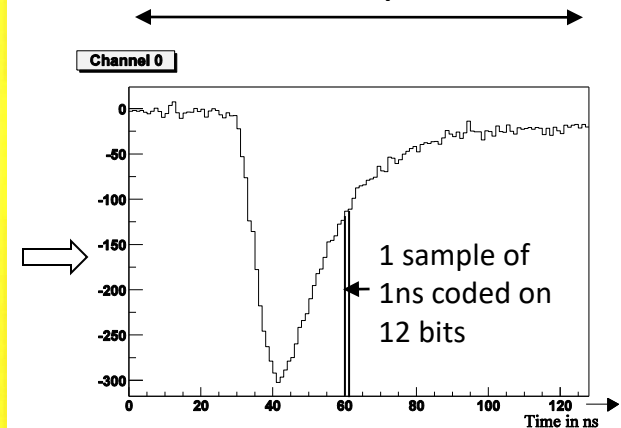
289 channels

PbF₂



Proton array signal

128 samples



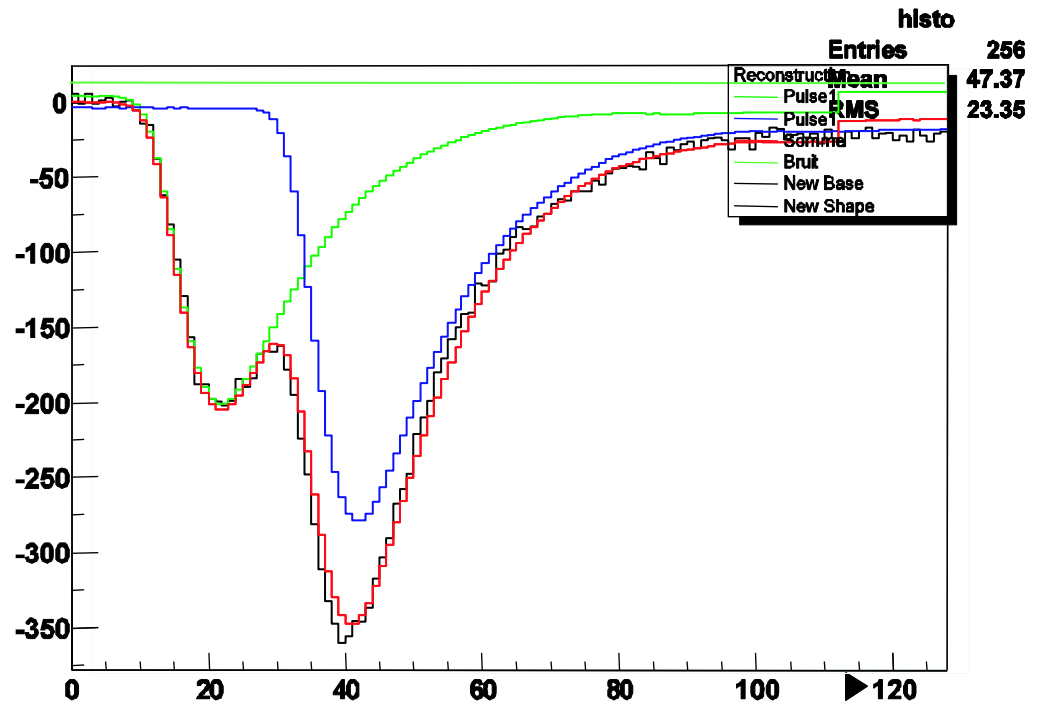
Equivalent to one digital oscilloscope put on each detector channel

Pile up events

Resolve pile up at
5 ns level

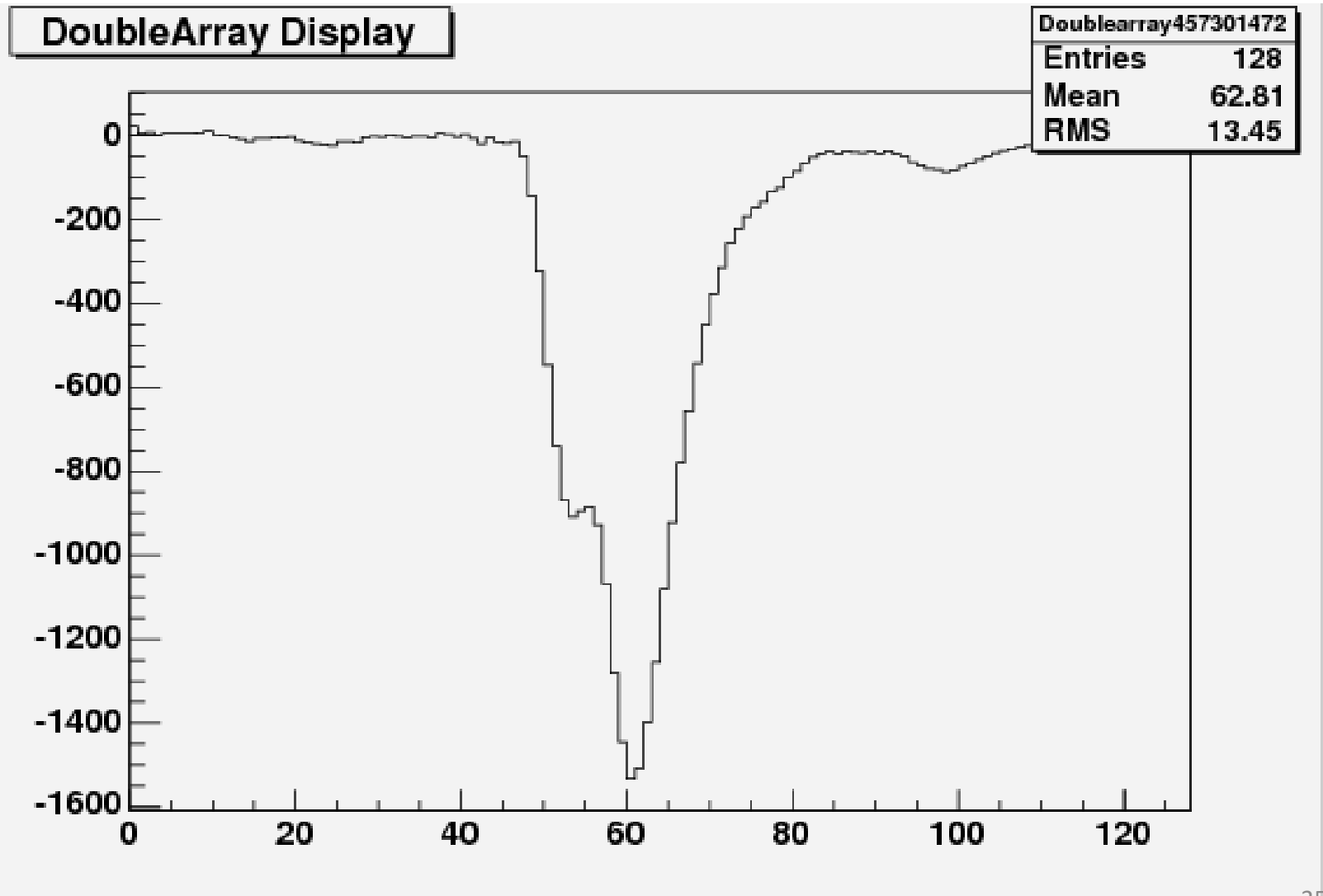
20% of events with
pile-up at 3 uA

Timing resolution
0.6 ns

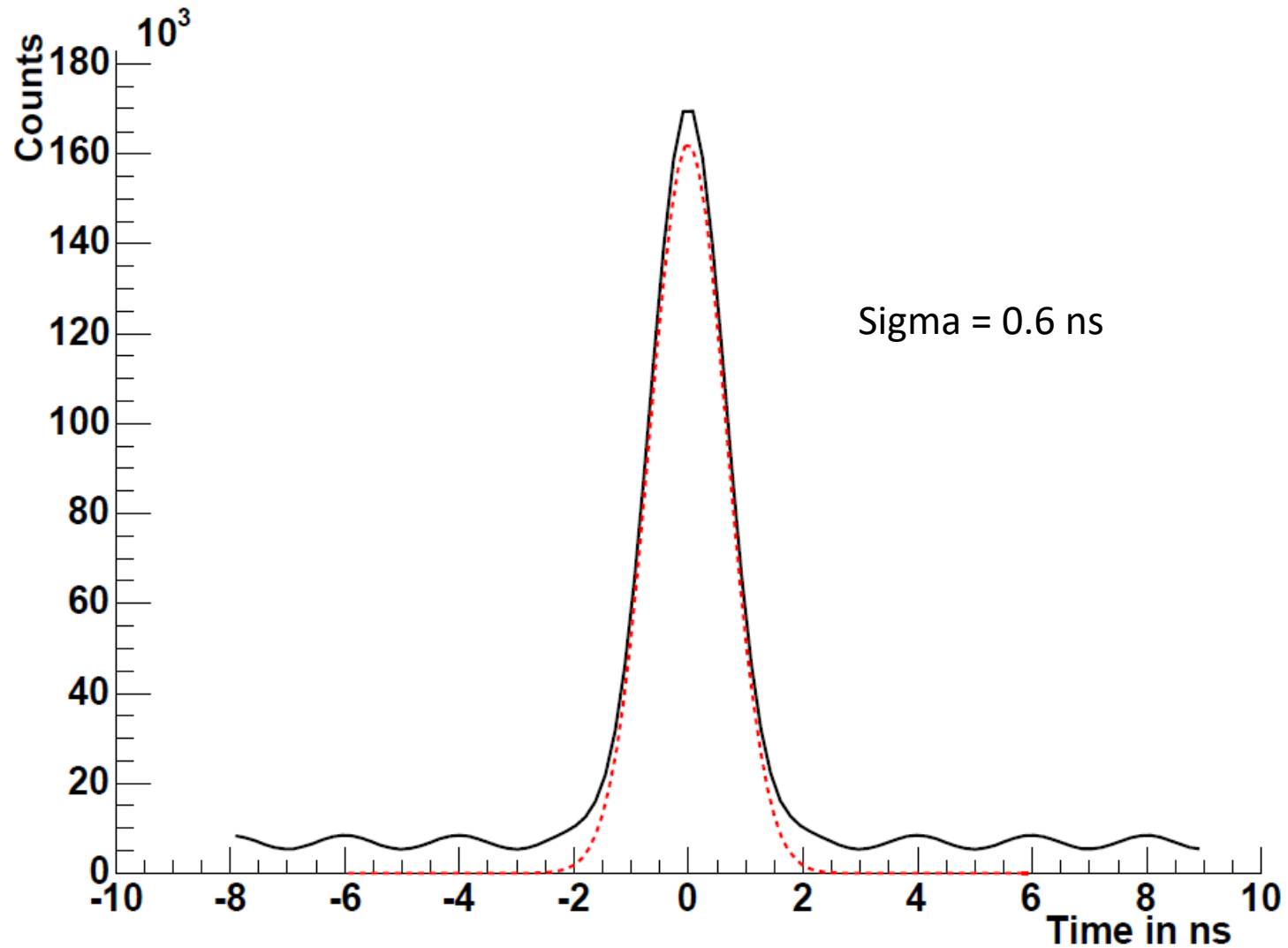


Singles rate in one block up to
1 MHz

Pile up calorimeter



Coincidence time

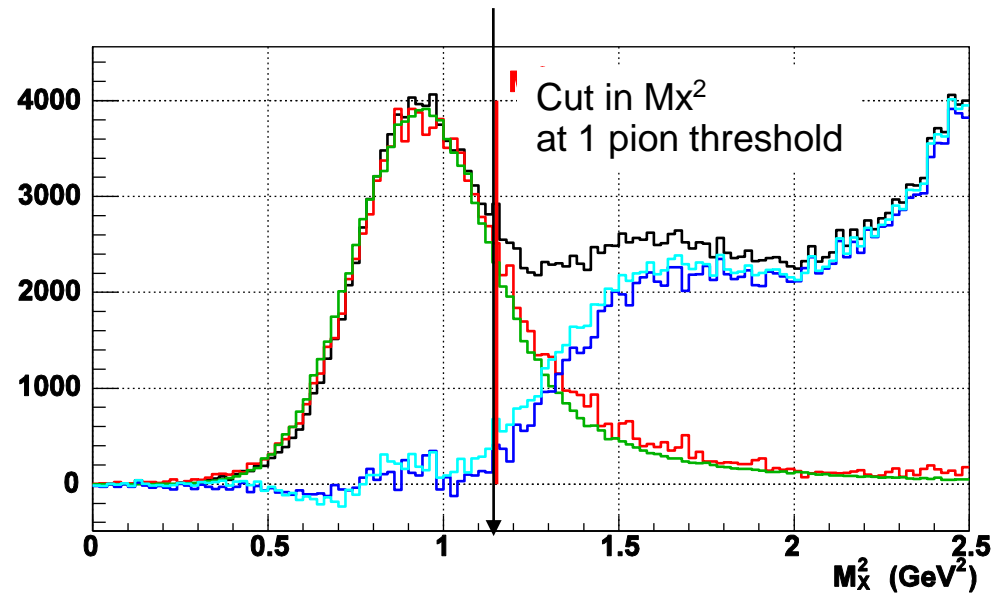
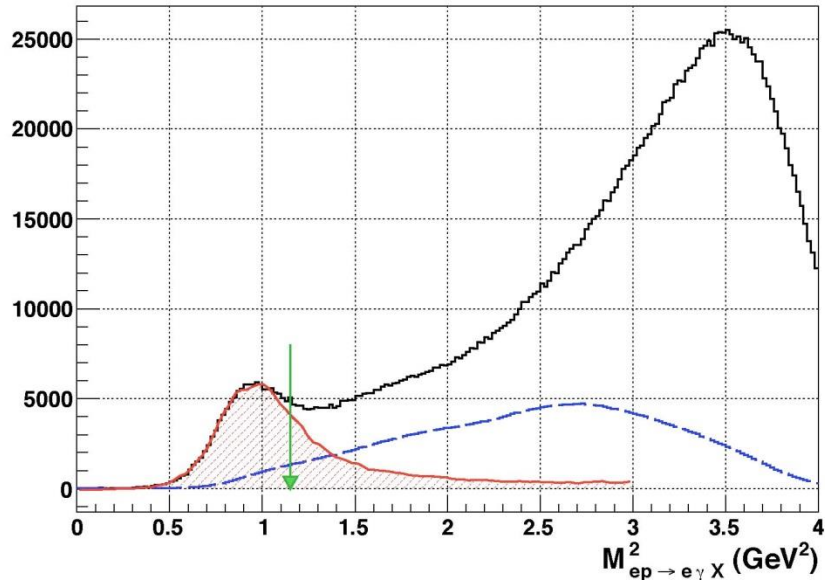


Data analysis proton DVCS

$$ep \rightarrow e\gamma X$$

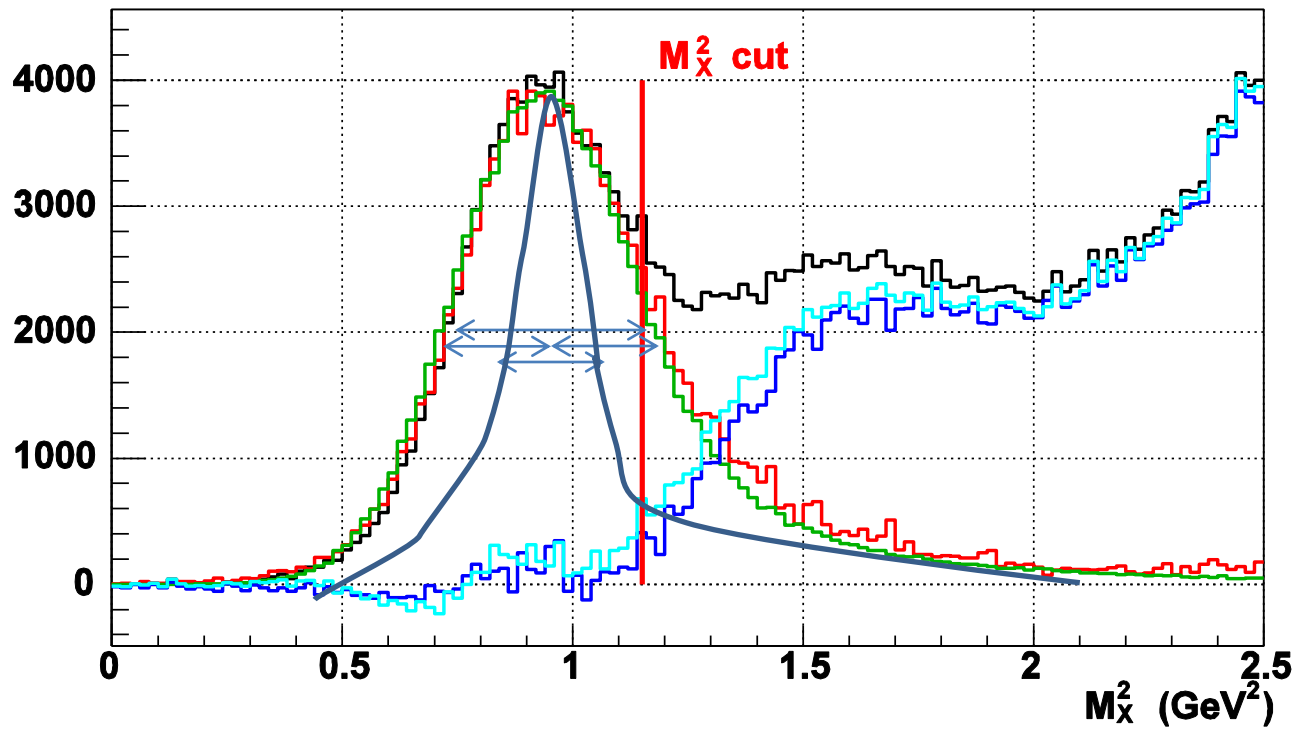
π^0 subtraction done using the π^0 sample recorded in the calorimeter

Subtracted data fits exactly the simulation and the shape of the exclusive events:
good understanding of the detectors
Exclusivity in two arms

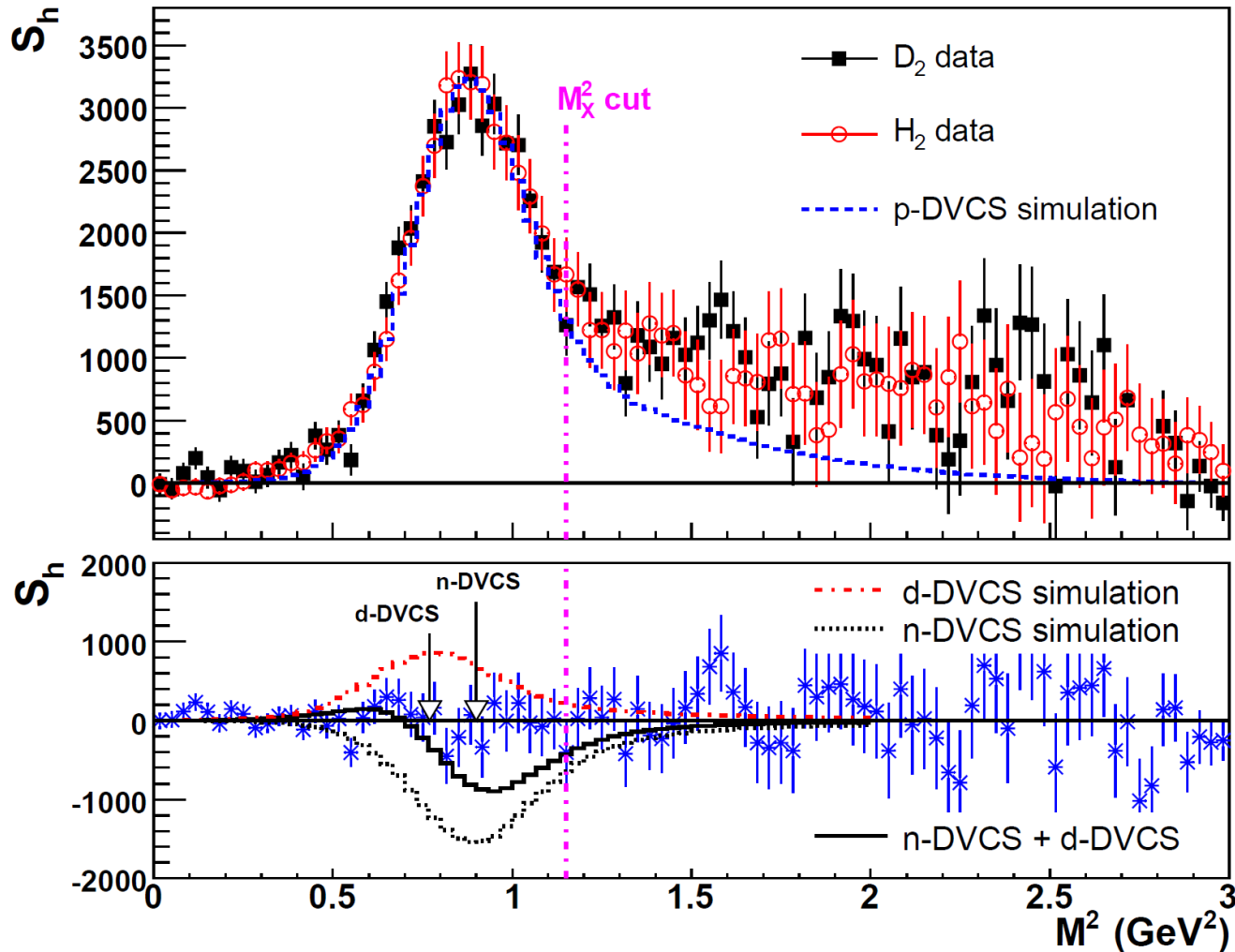


Missing mass resolution

- Driven by calorimeter resolution about 2000 photons
- Typical QE 25 %, if 100 % resolution twice better



Neutron DVCS in Hall A



- Hall A measurement done by subtraction of D data minus H data
- Possible contribution of the coherent deuteron which cannot be separated
- Need to tag the deuteron or better calorimeter resolution

Hall A/C DVCS experience

- 2005 experiment (3 μA)
 - Luminosity was limited by proton array pile up and DC current from low energy background
 - Uneven radiation damage of calorimeter
- 2010 experiment (5 to 10 μA)
 - Calorimeter only
 - Limited by pile up and DC current
 - Calorimeter crystal radiation damage
- 2016 experiment (5 to 10 μA)
 - Calorimeter only
 - Limited by pile up and DC current
 - Calorimeter crystal radiation damage
- 2023
 - Calorimeter only PbWO₄
 - Sweeping magnet

Detector aging

- Most detector based on ionization (GEM, PMTs, silicon detector) and charge multiplication have aging
 - Photocathode damage
 - Surface contamination of dynodes by ions reduces multiplication and gain drops with aging
- Radiation damage
 - Semiconductor junction can be damaged by radiation

Improvement needed for detector

- Shorter pulse : fastest PMT ~ 10 ns
- Good timing resolution (reduce pile-up and improve particle identification)
 - PMTs and scintillator : 100 ps
 - MRPC : 80 to 50 ps
 - Silicon strip : few ns
- Radiation hardness
- Long lifetime (no or little aging from signals)
- Costs (silicon detector are expensive)
- Good candidates:
 - MCP PMT (10 ps)
 - Expensive for large area : LAPPD being developed
 - Dead time
 - Determine aging : similar to PMTs
 - Superconducting detectors in cases where cryogenics is available

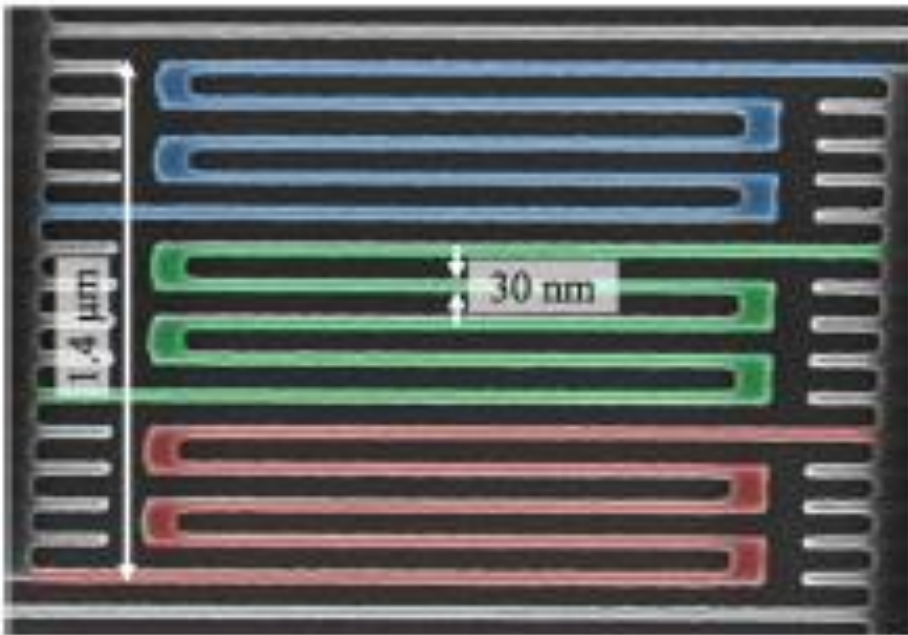
Superconductor

- When cooled down under critical Temperature T_c , electron tend to pair and can . Current can flow without seeing resistivity (no joule effect)
- Critical current : maximum current that can be carried by the superconductor. Transition to normal conducting above this current
- Temperatures from 4 K to 70 K
- Typically used at Jefferson Laboratory
 - Superconducting RF cavities
 - Superconducting magnets
 - Superconducting electronics and computers
 - Superconducting detectors

Superconducting detectors

	Two spectroscopic domains		
Type	Energy	Time	Temp.
Calorimeter TES, MMC...	Extremely high(1.2 eV)	Slow (ms)	< 0.1 K
STJ	High (3 - 6 eV)	Fast (μ s)	0.3 K
SSD (nano-strip)	N/A	Extremely fast (< 1 ns)	> 4.2 K

Single Superconducting Nanowire Photon Detectors (SNSPD)

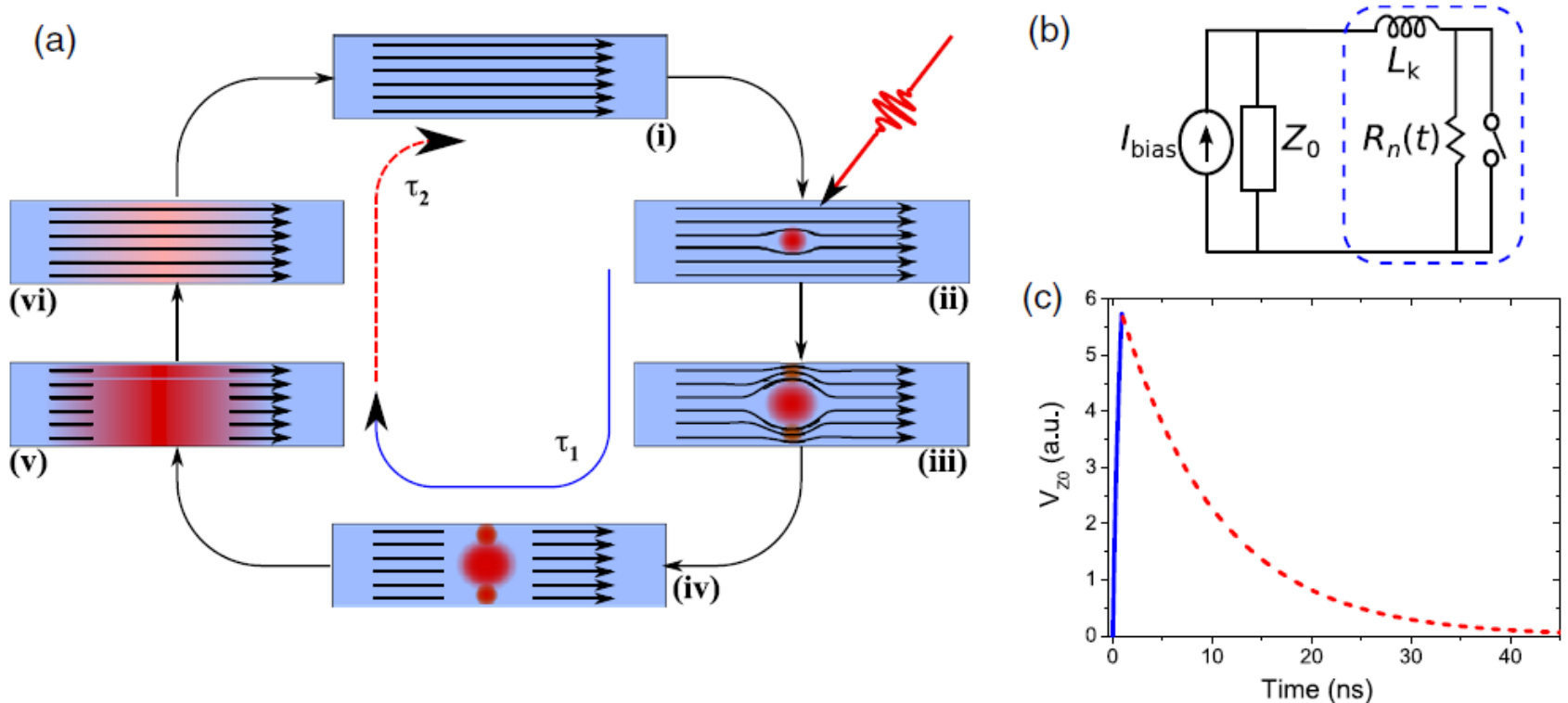


- Thin superconducting stripe of 5 to 10 nm thickness
- Meander geometry to maximize surface, typical width of strip 10 nm and length about 100 nm
- Signal speed depends on material, substrate and geometry

•Mostly developed for astrophysics with IR sensitivity : Nasa Jet Propulsion Laboratory, Lincoln Laboratory

Single Superconducting Nanowire Photon Detectors (SNSPD)

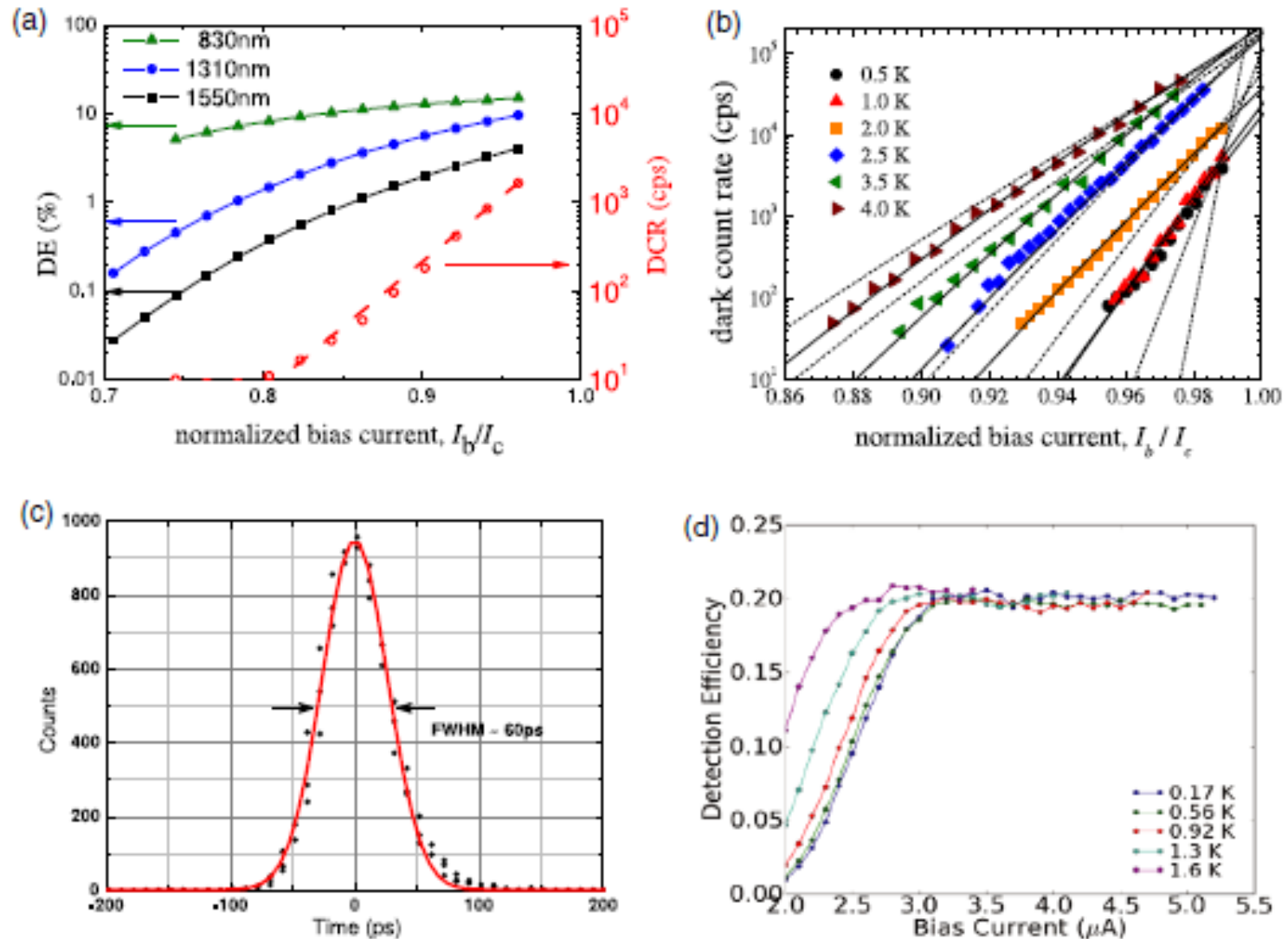
- Review : Chandra M Natarajan *et al* 2012 *Supercond. Sci. Technol.* **25** 063001 [doi:10.1088/0953-2048/25/6/063001](https://doi.org/10.1088/0953-2048/25/6/063001)



Features of SNSPD

- Fast
- Not based on ionization
- Sensitivity can be tuned by varying thickness and width of the strip (X-ray sensitivity to IR)
- Very good timing resolution
- Very small : very good position resolution
- No energy information

SNSPD typical properties



Superconductors properties

- L Parlato *et al* 2005 *Supercond. Sci. Technol.* **18** 1244 [doi:10.1088/0953-2048/18/9/018](https://doi.org/10.1088/0953-2048/18/9/018)

Metal	τ_0 (ns)	T_c (K)	T_D (K)	$2\Delta/kT_c$	10^3b (meV ⁻²)
Nb	0.37	9.2	276	3.92	1.55
Tc	0.609	7.8	411	3.48	0.57
V	1.71	5.4	380	3.45	0.61
Ta	1.88	4.47	240	3.45	1.66
Sn	2.24	3.75	200	3.66	2.40
In	0.77	3.4	108	3.69	9.90
Tl	1.26	2.33	78	3.69	18.6
Re	92.5	1.697	415	3.38	0.36
Al	395	1.196	428	3.34	0.35
Mo	748	0.915	460	3.53	0.29
Zn	556	0.875	327	3.19	0.59
Os	2480	0.66	500	—	0.23
Zr	996	0.61	290	—	0.73
Ru	9220	0.49	600	3.42	0.15
Ti	7960	0.4	415	3.43	0.32
Hf	95700	0.128	252	3.63	0.82
Ir	414000	0.1125	420	—	0.28

Compound	T_c (K)	T_D (K)	10^3b (meV ⁻²)	τ_0 (ns)
MgB ₂ ^a	39	442	1.13	0.002
NbB ₂ ^b	0.62	325	0.57	1207

Compound	T_c (K)	T_D (K)	10^3b (meV ⁻²)	τ_0 (ns)
NbN ^a	15	400	0.78	0.06
ZrN _{0.98} ^b	10	360	0.85	0.19
VN ^c	8.5	465	0.44	0.61
TiN _{0.98} ^d	4.6	480	0.35	4.87

Alloy	τ_0 (ns)	T_c (K)	T_D (K)	10^3b (meV ⁻²)
Mo _{0.18} Tc _{0.82}	0.08	13.7	385	0.82
Mo _{0.18} Tc _{0.82}	0.08	13.7	385	0.82
Mo _{0.6} Re _{0.4}	0.08	12.6	340	1.07
Mo _{0.7} Re _{0.3}	0.19	10.8	395	0.70
Zr _{0.1} Nb _{0.9}	0.05	10.5	220	2.91
Mo _{0.23} Re _{0.77}	0.13	9.25	272	1.61
Mo _{0.8} Re _{0.2}	0.48	8.5	420	0.56
Ti _{0.25} V _{0.75}	0.33	7.16	279	1.37
Ti _{0.15} V _{0.85}	0.36	7.02	283	1.31
W _{0.65} Re _{0.35}	0.51	6.75	309	1.05
Mo _{0.4} Re _{0.6}	0.80	6.49	355	0.75
Mo _{0.42} Re _{0.58}	0.84	6.35	351	0.77
Nb _{0.9} Mo _{0.1}	0.86	5.3	275	1.28
W _{0.59} Re _{0.50}	1.44	5.12	327	0.85
Ti _{0.8} V _{0.2}	2.37	3.5	235	1.62
Mo _{0.9} Re _{0.1}	17.7	2.9	440	0.38
Mo _{0.95} Re _{0.05}	151	1.5	450	0.32
Os _{0.4} Ir _{0.6}	1139	0.74	410	0.36

YBaCuO

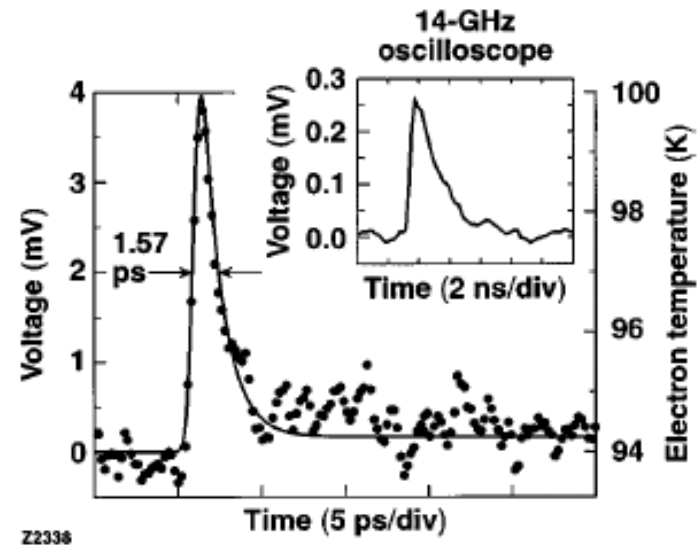
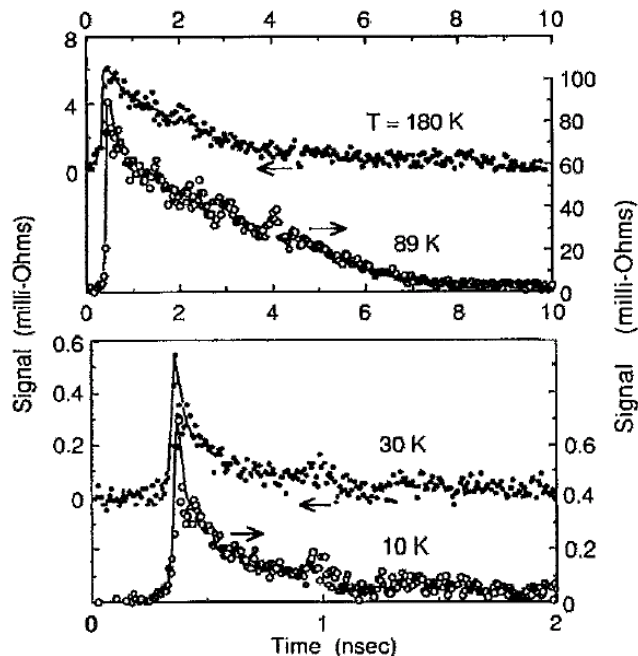
- **Nonbolometric photoresponse of YBa₂Cu₃O₇ films**

Mark Johnson

Citation: Applied Physics Letters **59**, 1371 (1991); doi: 10.1063/1.105312

- **Intrinsic picosecond response times of Y–Ba–Cu–O superconducting photodetectors**

M. Lindgren, M. Currie, C. Williams, T. Y. Hsiang, P. M. Fauchet, Roman Sobolewski, S. H. Moffat, R. A. Hughes, J. S. Preston, and F. A. Hegmann
Applied Physics Letters **74**, 853 (1999); doi: 10.1063/1.123388



Picosecond timing measurement

- **Real-time measurement of picosecond THz pulses by an ultra-fast YBa2Cu3O7-d detection system**
- P. Thoma, A. Scheuring, M. Hofherr, S. Wünsch, K. Il'in, N. Smale, V. Judin, N. Hiller, A.-S. Müller, A. Semenov,
- H.-W. Hübers, and M. Siegel
- Citation: Applied Physics Letters **101**, 142601 (2012); doi: 10.1063/1.4756905

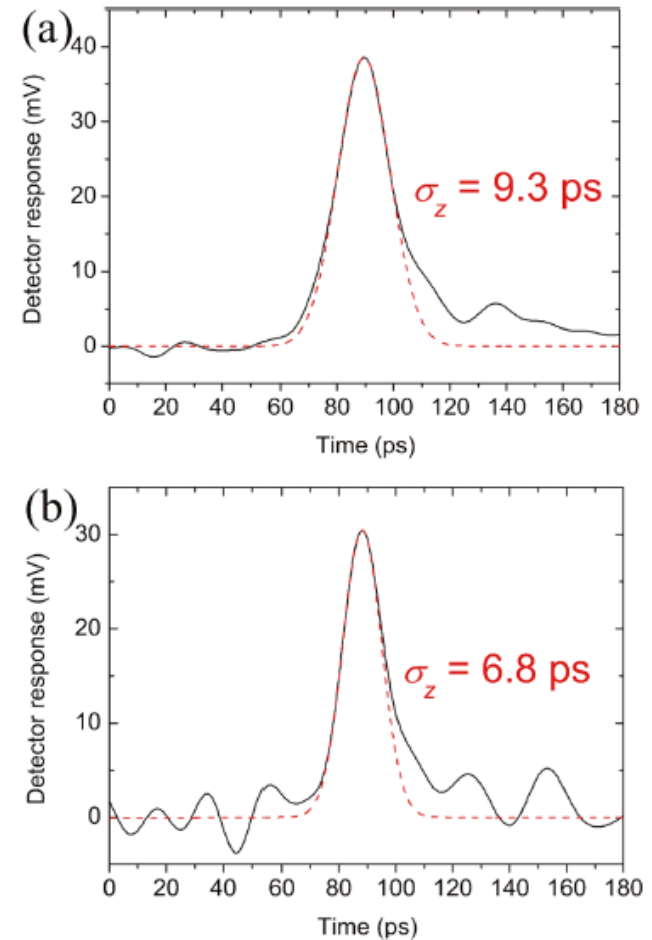
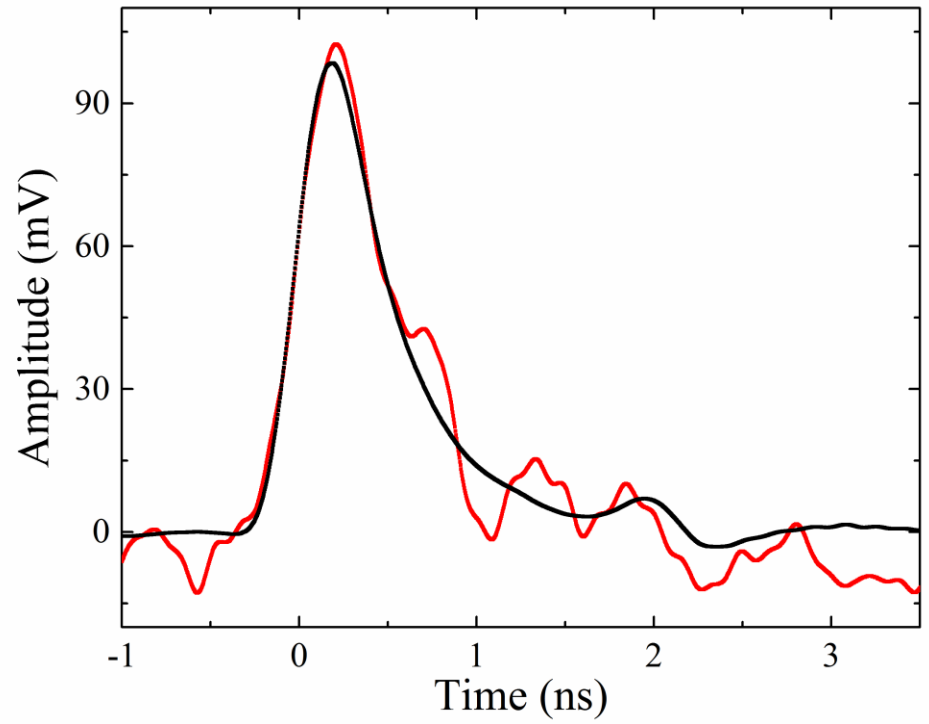
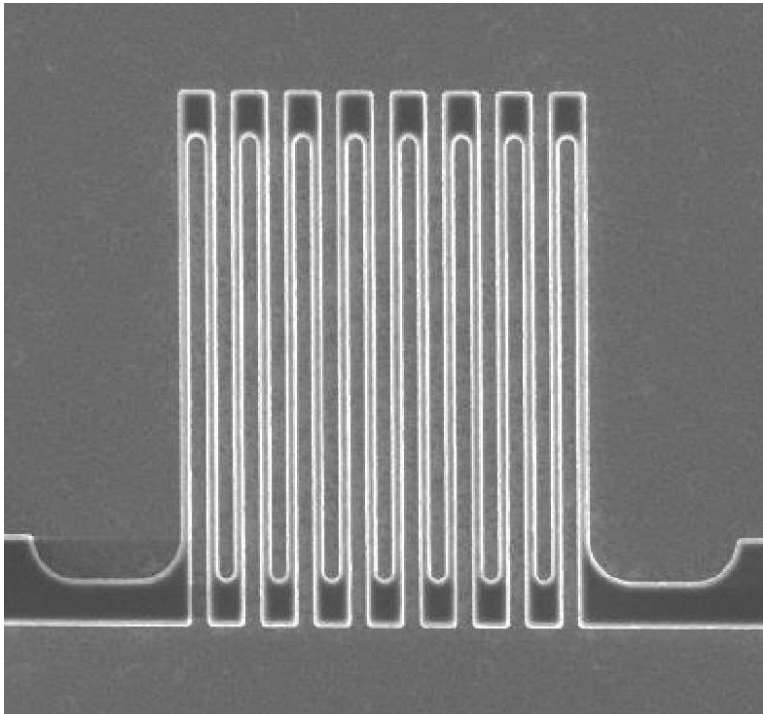


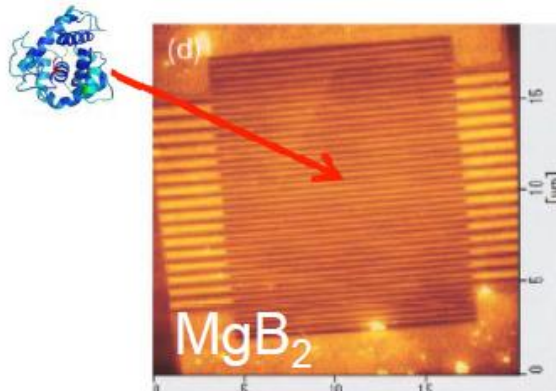
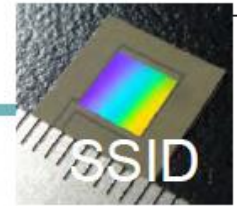
FIG. 3. (a) Averaged YBCO detector response (solid line) of 20 single shots. The rms pulse length was determined by a Gaussian fit (dashed line) to 9.3 ps. (b) Single shot of the YBCO detector system. Pulse lengths as short as 6.8 ps were recorded.

MgB2

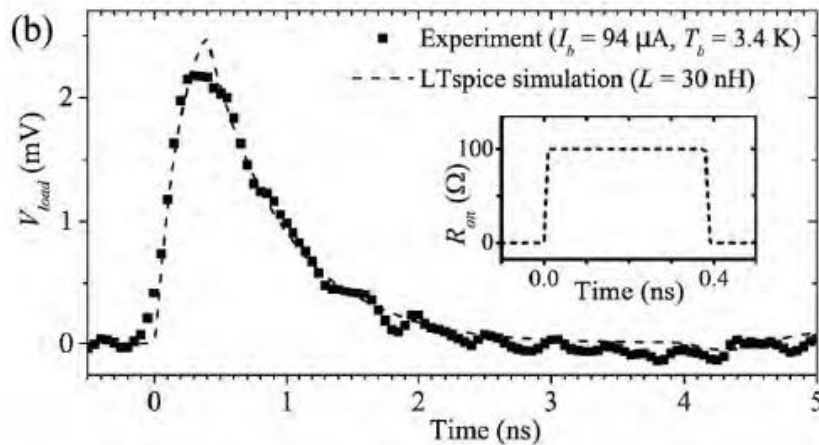
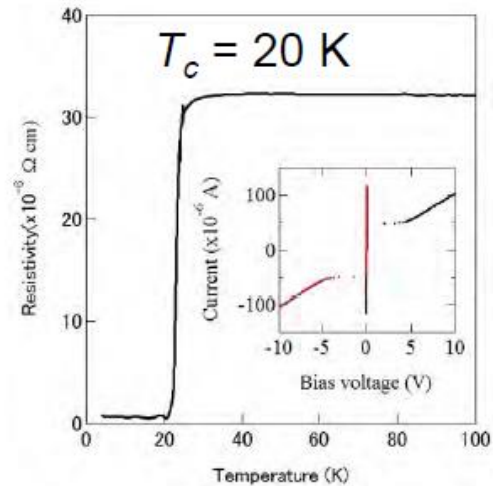


JPL F. Marsili

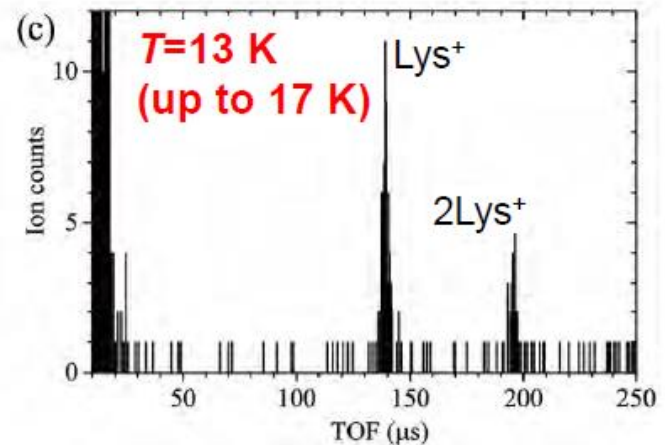
Detection of lysozyme ions with MgB₂-SSID



$d = 10 \text{ nm}$, $w = 250 \text{ nm}$ (2 nm-AlN)
 $10 \times 10 \mu\text{m}^2$, $I_c = 96 \text{ A}$

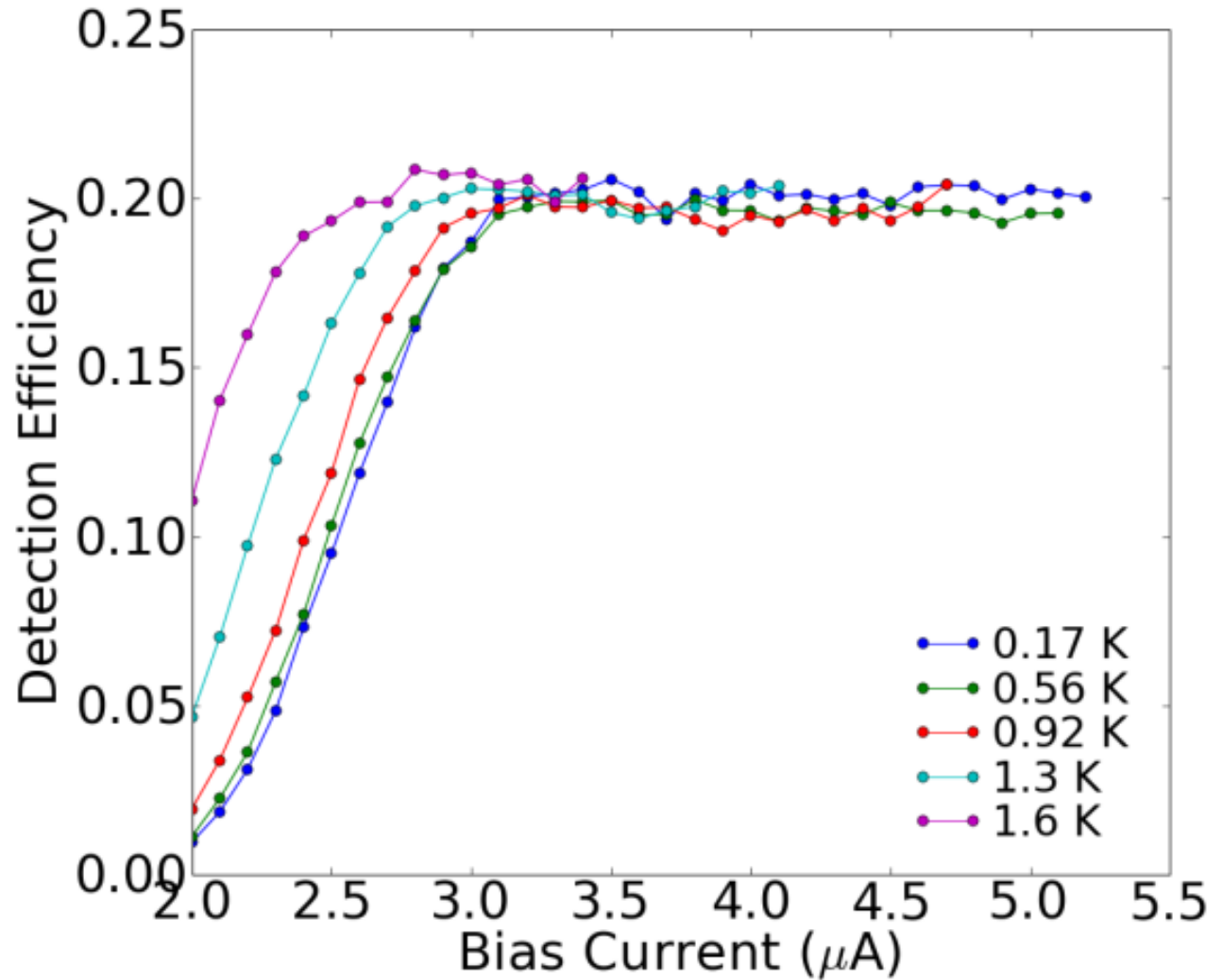
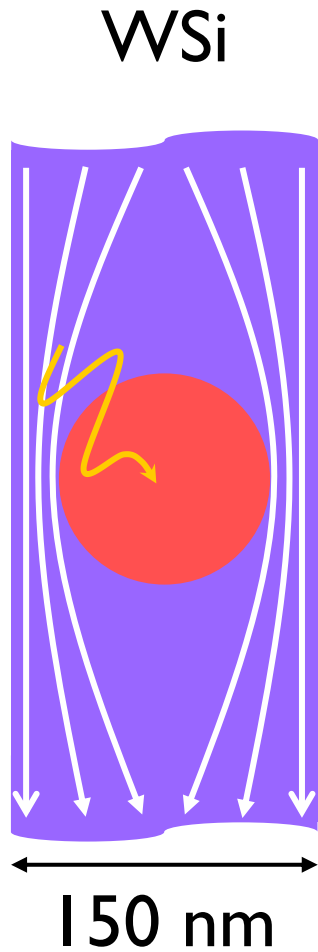


LTspice can reproduce the pulse shape.



Mass spectrum was obtained.

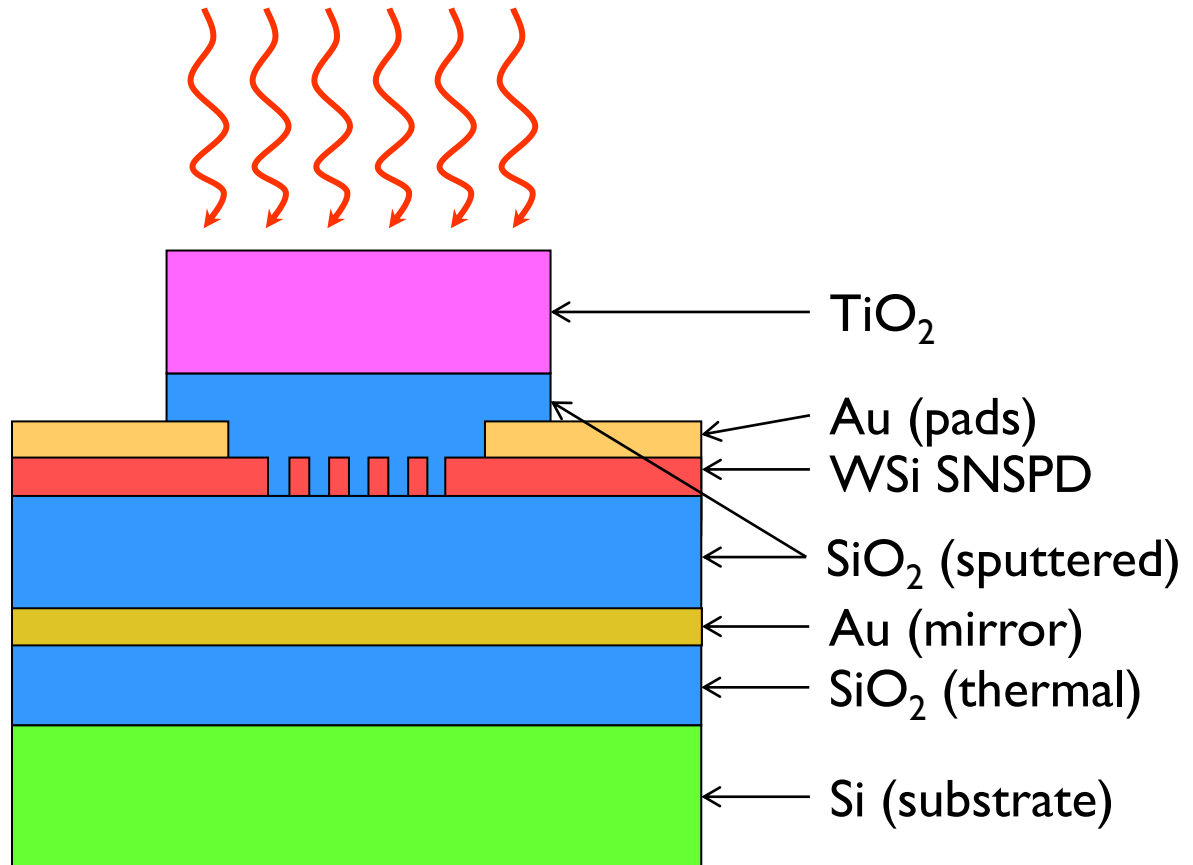
WSi



WSi

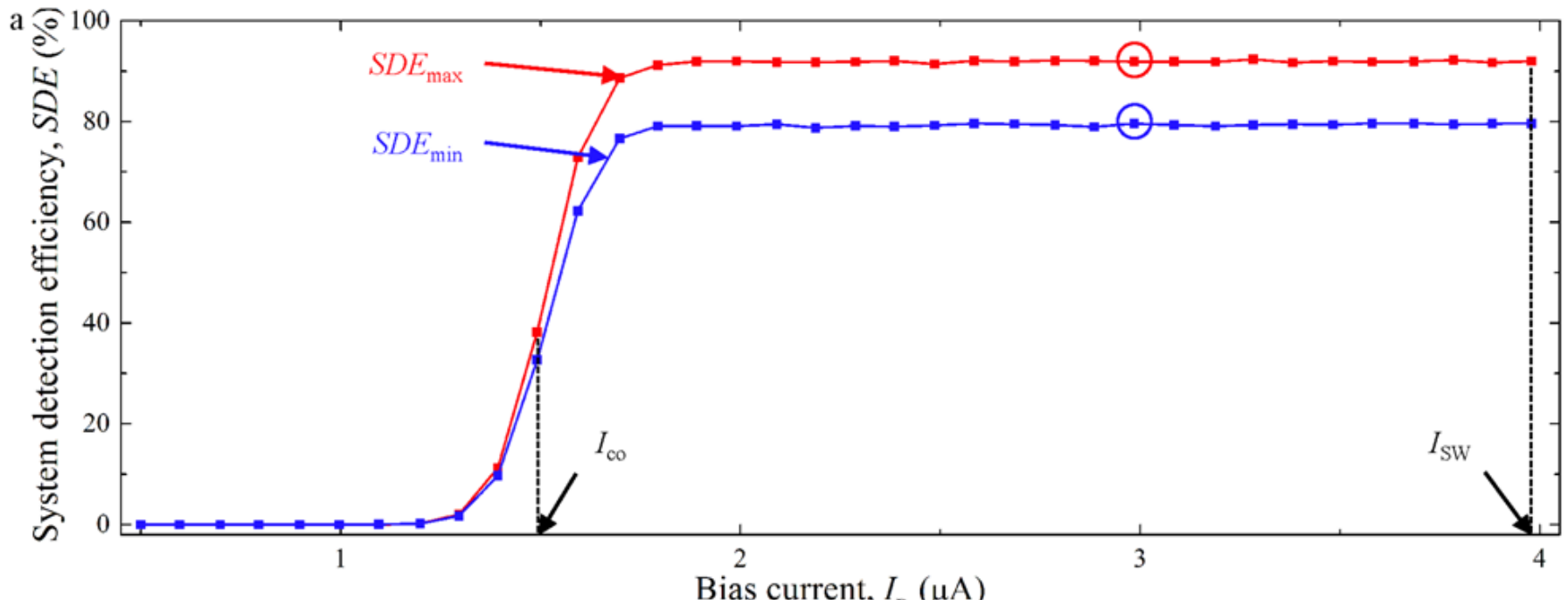
Operating
temperature
1 K

Add optical cavity to
improve detection
efficiency



WSi

93 % detection efficiency




Fabrication process

- Similar to microelectronics
 - Metal deposition
 - Lithography
 - Etching

Metal deposition

- Sputtering process
- Process being developed at Jefferson Laboratory
- (Superconducting Radio Frequency group)
Anne-Marie Valente Feliciano

Superconducting Thin Films



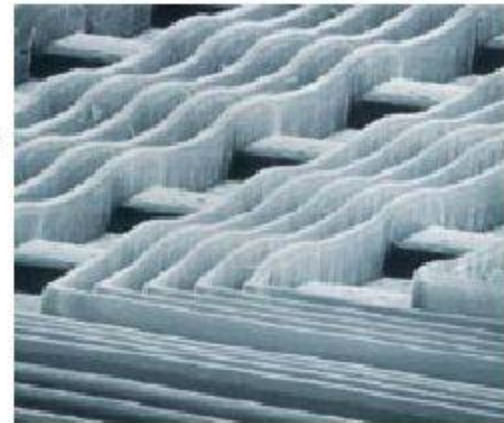
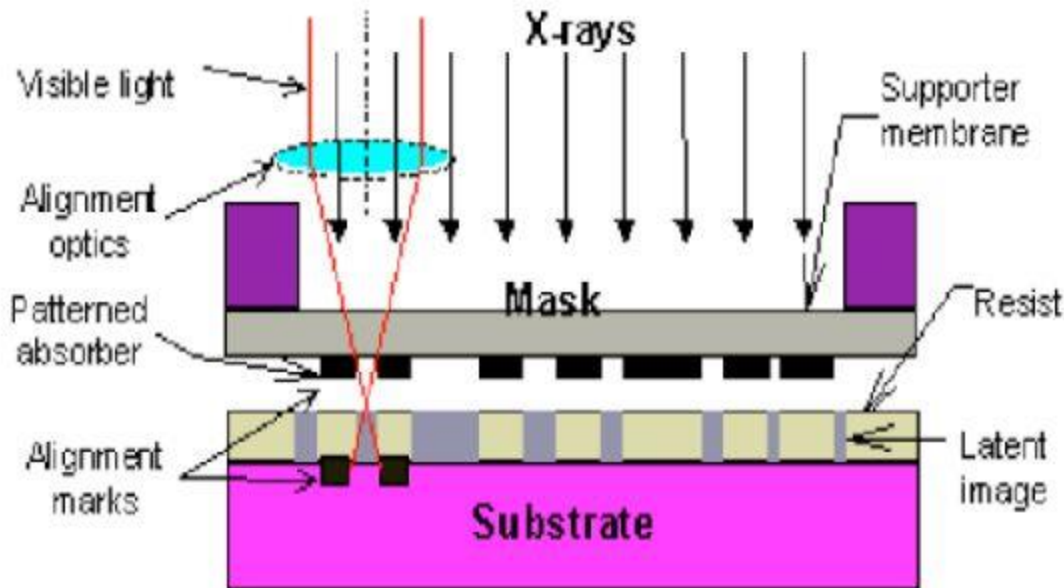
Base pressure without baking
 2×10^{-9} Torr
UV desorption system
NEG chamber
3 magnetrons (DC, RF)
Self-sputtered magnetron
Ion source
RGA chamber with differential
pumping
Thickness monitors

4/14/2010

4/14/2010

Lithography techniques

- Visible / UV optical lithography
- Electron beam lithography
- X-ray lithography
- X-ray diffraction lithography



Films and Lithography session

Monday November 28th 2022

13:00

Superconducting thin films developements

Anne-Marie Valente-Feliciano

F113, Thomas Jefferson National Accererator Facility Cebaf Center

13:00 - 13:45

Nb3Sn thin films

Uttar Pudasaini

14:00

F113, Thomas Jefferson National Accererator Facility Cebaf Center

13:45 - 14:15

IARPA C3 and SuperTools projects summary

Douglas Scott Holmes

F113, Thomas Jefferson National Accererator Facility Cebaf Center

14:15 - 14:50

Superconducting electronics

- Detectors are fast, need fast electronics to take advantage of the speed
- Small pixels give better timing and position resolutions but need to handle billions of pixels
- Detectors will be in Helium bath, integrated superconducting electronics can reduce the number of connections going out

Superconducting electronics session

Tue 29/11

09:00	Josephson Junction based Quantum Computing <i>F113, Thomas Jefferson National Accelerator Facility Cebaf Center</i>	<i>Briton Plourde</i> 09:00 - 09:30
	The EIC on a Table Top <i>F113, Thomas Jefferson National Accelerator Facility Cebaf Center</i>	<i>Robert Edwards</i> 09:30 - 10:00
10:00	Dune cryogenics electronics <i>F113, Thomas Jefferson National Accelerator Facility Cebaf Center</i>	<i>Hanjie Liu</i> 10:00 - 10:30
	Coffee break <i>F113, Thomas Jefferson National Accelerator Facility Cebaf Center</i>	10:30 - 11:00
11:00	Cryogenics ASICs at Fermilab <i>F113, Thomas Jefferson National Accelerator Facility Cebaf Center</i>	<i>Dr Davide Braga</i> 11:00 - 11:30
	CAEN Electronics readout <i>F113, Thomas Jefferson National Accelerator Facility Cebaf Center</i>	<i>Carlo Tintori</i> 11:30 - 12:00
12:00		

Superconducting electronics

- More convenient to have close to detector
 - Amplify signal
 - Improve signal to noise
 - Interface with standard electronics
 - Very high density of detector (typical surface 100 nm x 100 nm)
- Performance superior to standard electronics
 - 19.6 GHz FADC
 - Subpicosecond achievable

Analog to Digital Converter

High-resolution ADC operation up to 19.6 GHz clock frequency

O A Mukhanov¹, V K Semenov², I V Vernik¹, A M Kadin¹,
T V Filippov², D Gupta¹, D K Brock¹, I Rochwarger¹ and
Y A Polyakov²

¹HYPRES, Inc, 175 Clearbrook Road, Elmsford, NY 10523, USA

²Physics Department, SUNY at Stony Brook, NY 11794, USA

Received 25 July 2001

Published 21 November 2001

Online at stacks.iop.org/SUST/14/1065

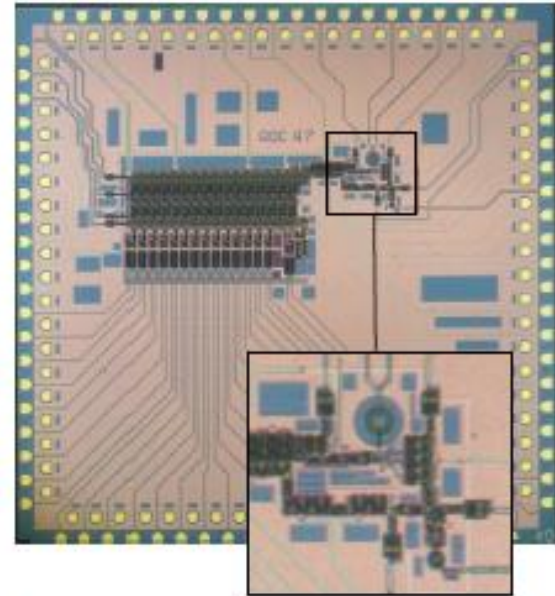


Figure 1. A 15-bit 2G ADC chip with a two-channel synchronizer. The inset shows the ADC front-end (modulator). The 6000-junction chip was fabricated using HYPRES' standard 1 kA cm^{-2} process with a $3 \text{ }\mu\text{m}$ minimum junction size.

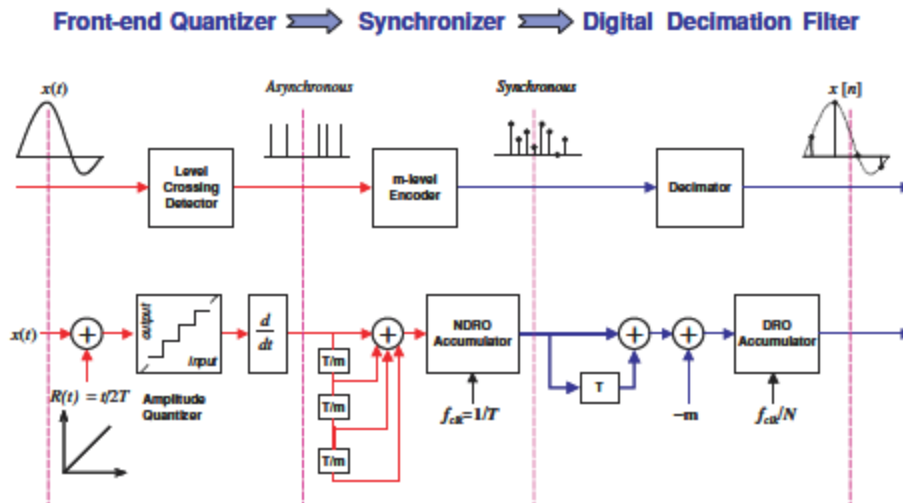


Figure 6. Functional model of our ADC based on phase modulation–demodulation architecture.

Rapid Flux Single Quantum electronics

- In a superconducting loop, magnetic flux is quantized hence the current, those unit are used as based to RFSQ electronics
- <http://www.hypres.com>
 - Clock
Dmitri E. Kirichenko and Igor V. Vernik, “High Quality On-Chip Long Annular Josephson Junction Clock Source for Digital Superconducting Electronics,” IEEE Trans. Appl. Supercond., 15, 296-299, June 2005
 - ADC
O. A. Mukhanov, V. K. Semenov, I. V. Vernik, A. M. Kadin, D. Gupta, D. K. Brock, I. Rochwarger, T. V. Filippov, and Y. A. Polyakov, “High resolution ADC operating up to 19.6 GHz clock frequency,” Supercond. Sci. Technolol. 14, 1065-1070, 2001.
 - TDCs
A. F. Kirichenko, S. Sarwana, O. A. Mukhanov, I. V. Vernik, Y. Zhang, J. H. Kang, and J. M. Vogt, “RSFQ Time Digitizing System,” IEEE Trans. Appl. Supercond., vol. 11, no. 1, pp. 978-981, Mar. 2001.

Detectors application

- Cerenkov based detectors : RICH and time of flight
- PMT replacement
- Scintillator based detectors

- Minimum ionizing particle tracker

- Liquid Helium detector

SNSPD as photodetector

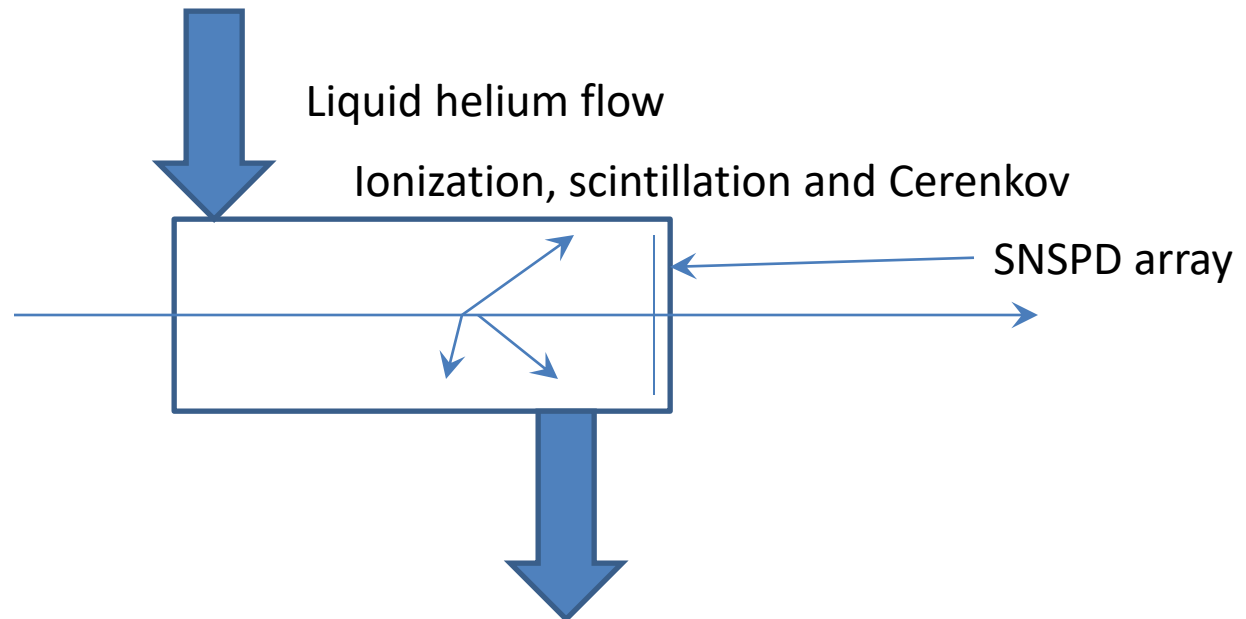
- PMT replacement
- Use radiator preferably Cerenkov for fastest response
- Typically, thickness being very small detector is insensitive to minimum ionizing particles
- Sensitive thickness of the order of 10 nanometers, thickness driven by substrate and can be reduced with respect to other detectors
- Need high pixellization for photon counting

Photon counting device : Pixellized SNSPDs

- Need to find a good way to reproduce same pattern
 - Optical lithography
 - X-ray
 - UV
 - Interferometric
 - Electron beam assisted deposition
 - Ion beam assisted deposition
 - Nano Imprint
- Need to be fast and cheap to compete with PMT

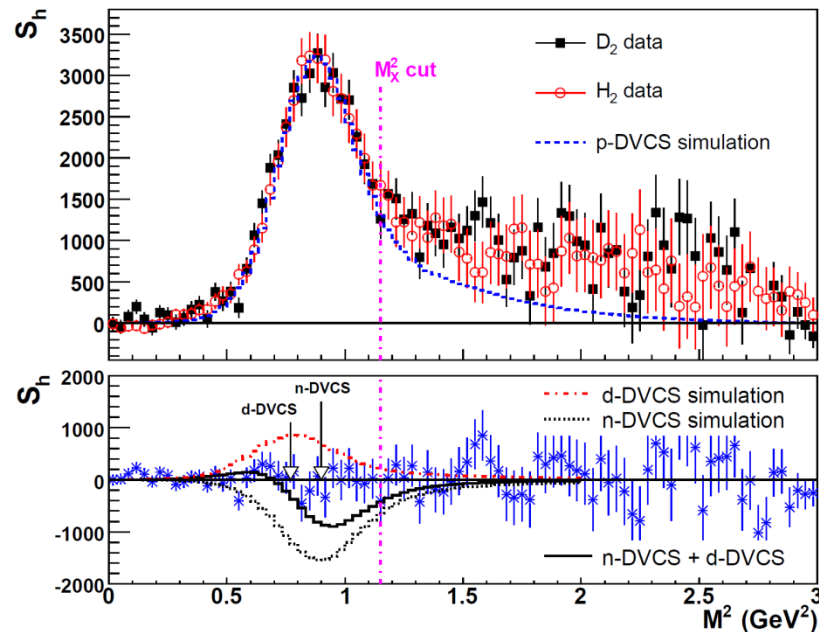
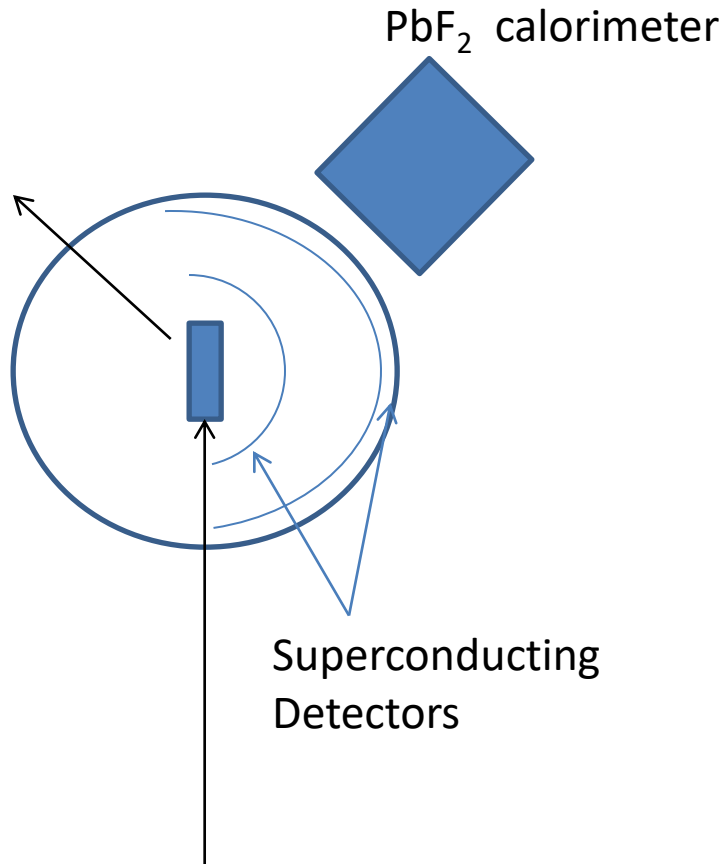
Liquid Helium detector

- Helium has very fast UV scintillation and slower component
- Helium is transparent to UV
- RICH + scintillation + Time of flight



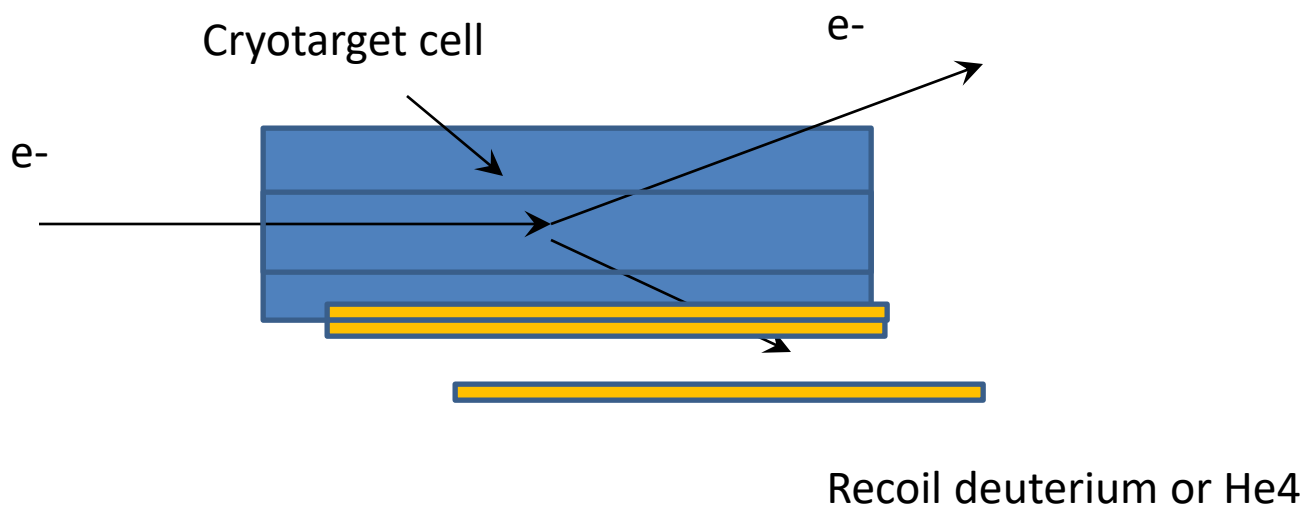
Improved Hall A nDVCS

- Detector in vacuum chamber
- Thickness minimized to detect deuterons
- Deutons which stop will be detected
- Use helium scintillation to estimate DE and E for PID
- Two layers for time of flight
- Calorimeter readout with SNSPD would have almost twice better resolution



Recoil detector for coherent DVCS

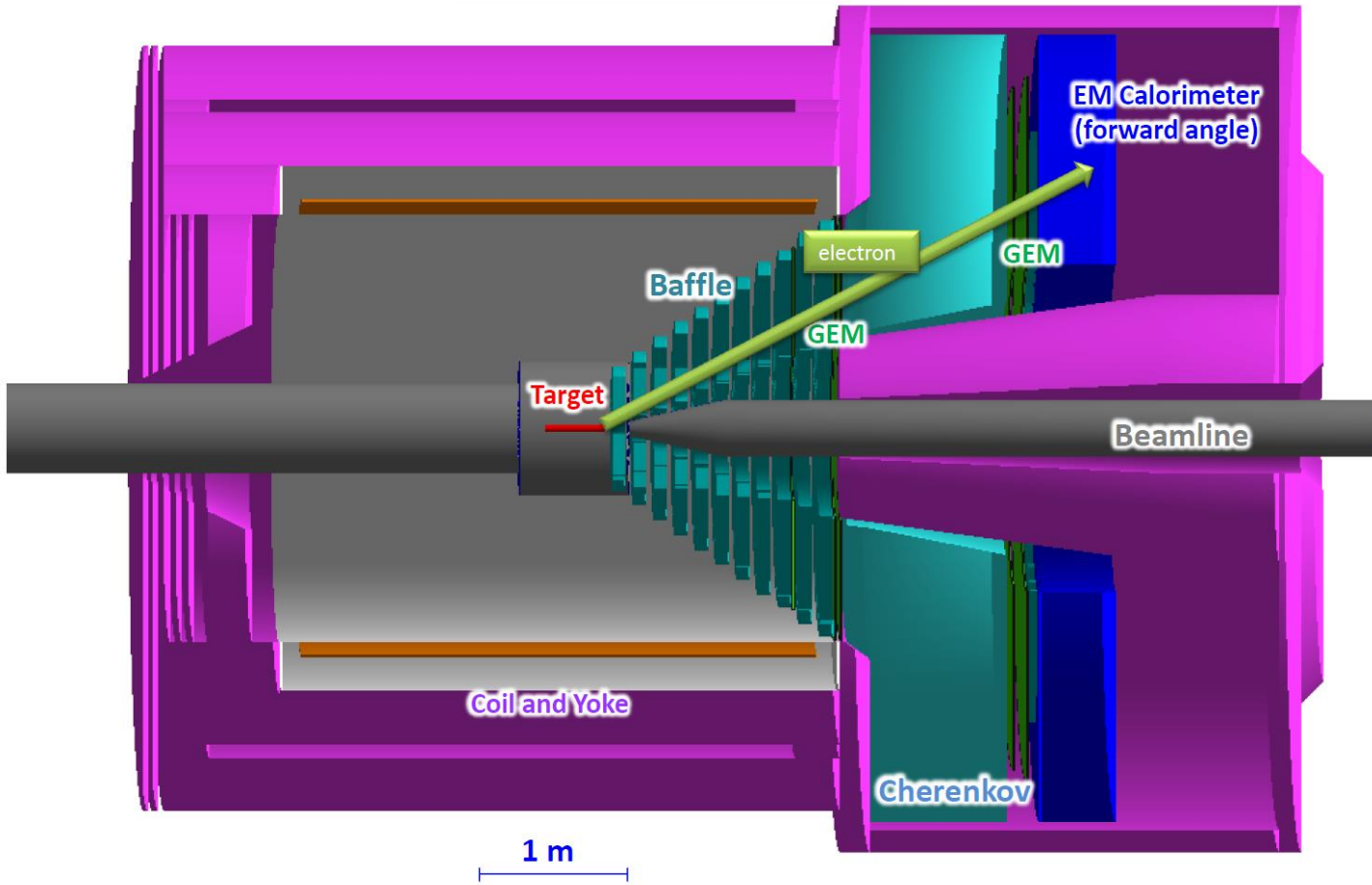
- $\gamma^* + D \longrightarrow D + \gamma$
- $\gamma^* + \text{He4} \longrightarrow \text{He4} + \gamma$



- Can use target as detector cooling : detector inside of target for very low momentum coherent nuclei
- Deuterium trickier than He4 because $T \sim 22\text{K}$

Detector layout and trigger for PVDIS

SoLID (PVDIS)



Trigger

Calorimeter and Gas Cerenkov

200 to 500 KHz of electrons

30 individual sectors to reduce rate

Max 30 KHz/sector

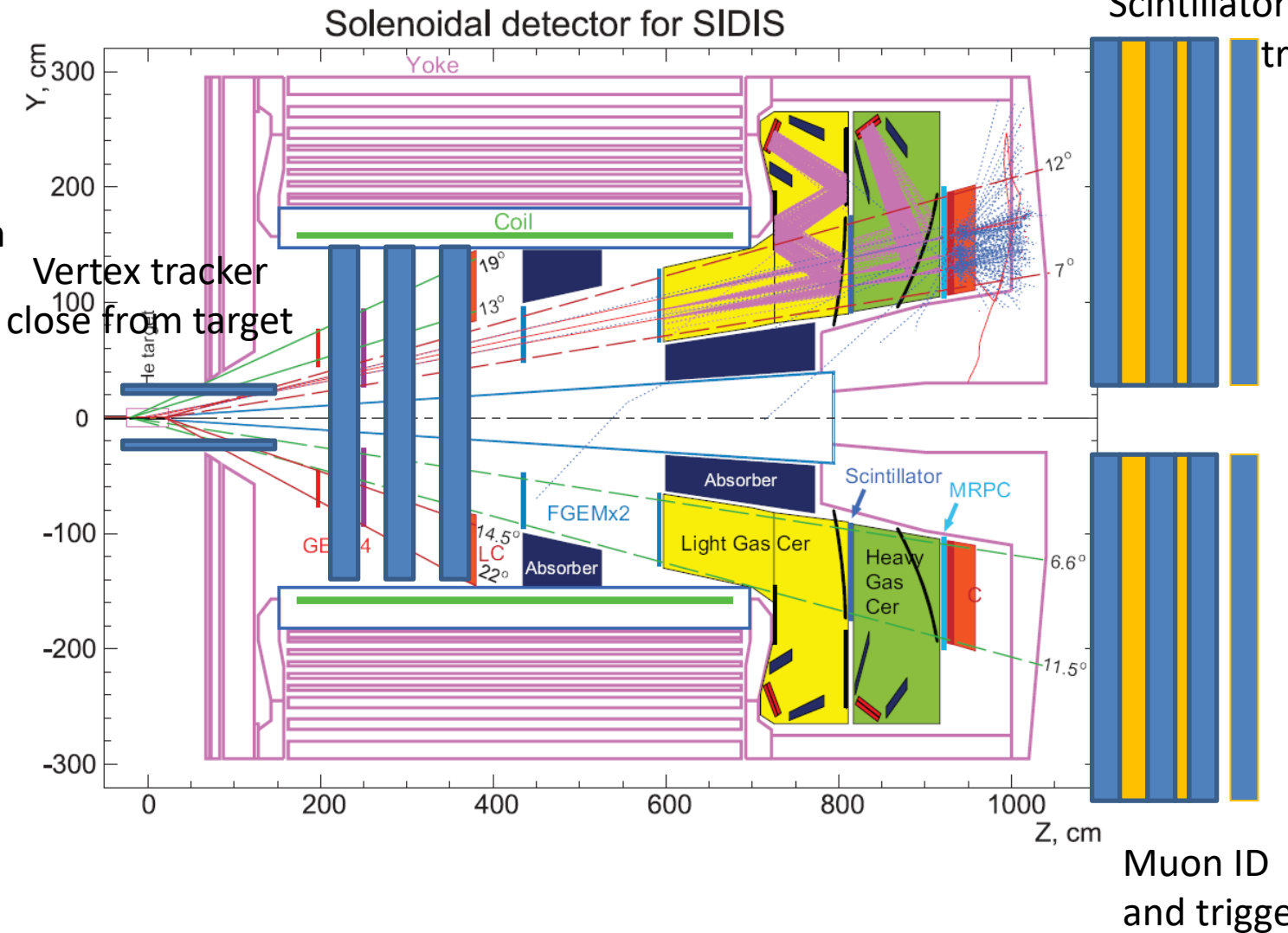
$10^{39} \text{ cm}^{-2} \text{ s}^{-1}$

SoLID DDVCS layout

J/psi
 3 uA on 15 cm LH2
 $10^{37} \text{ cm}^{-2} \text{ s}^{-1}$
 Detector limited

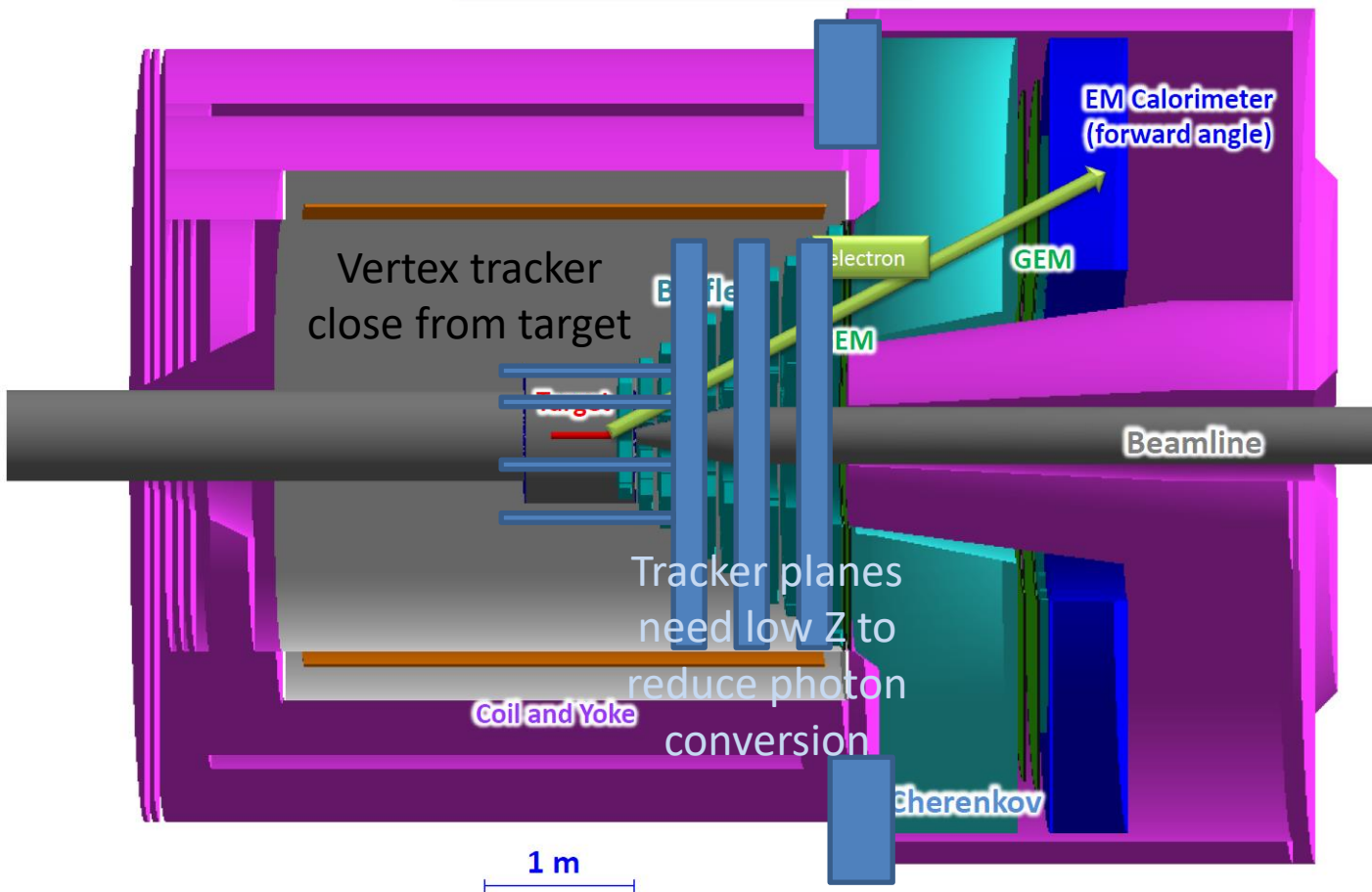
Could go up to 40 cm
 And 80 uA increase
 by about 60

Low mass detector
 less
 sensitive
 to photons



Detector layout and trigger for PVDIS

SoLID (PVDIS)



Remove baffle

Add materials

Tracker planes need low Z to reduce photon conversion

Replace PMT for Cerenkov by SNSPD to improve rate capability

MOLLER and SoLID

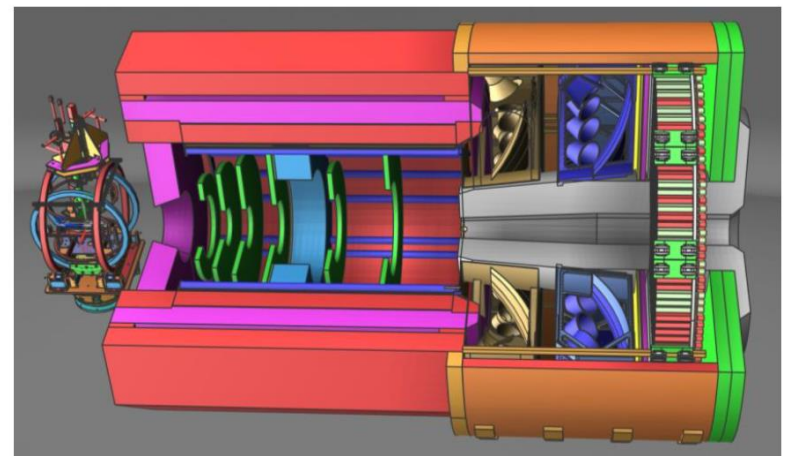
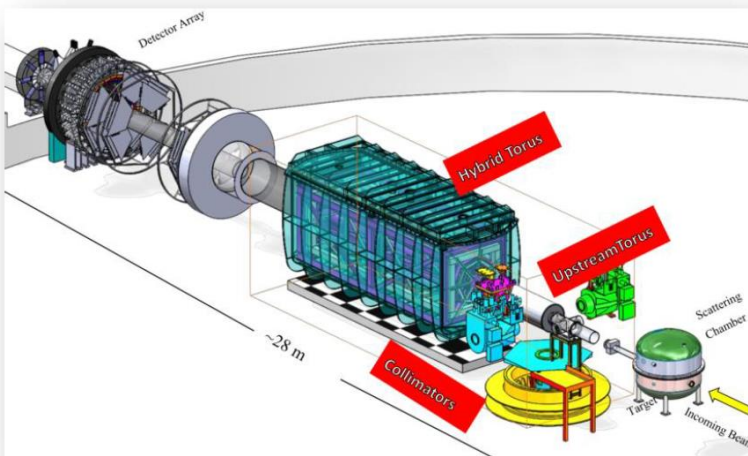
- Two projects that take advantage of 12 GeV CEBAF capabilities and will make the most of that investment

MOLLER

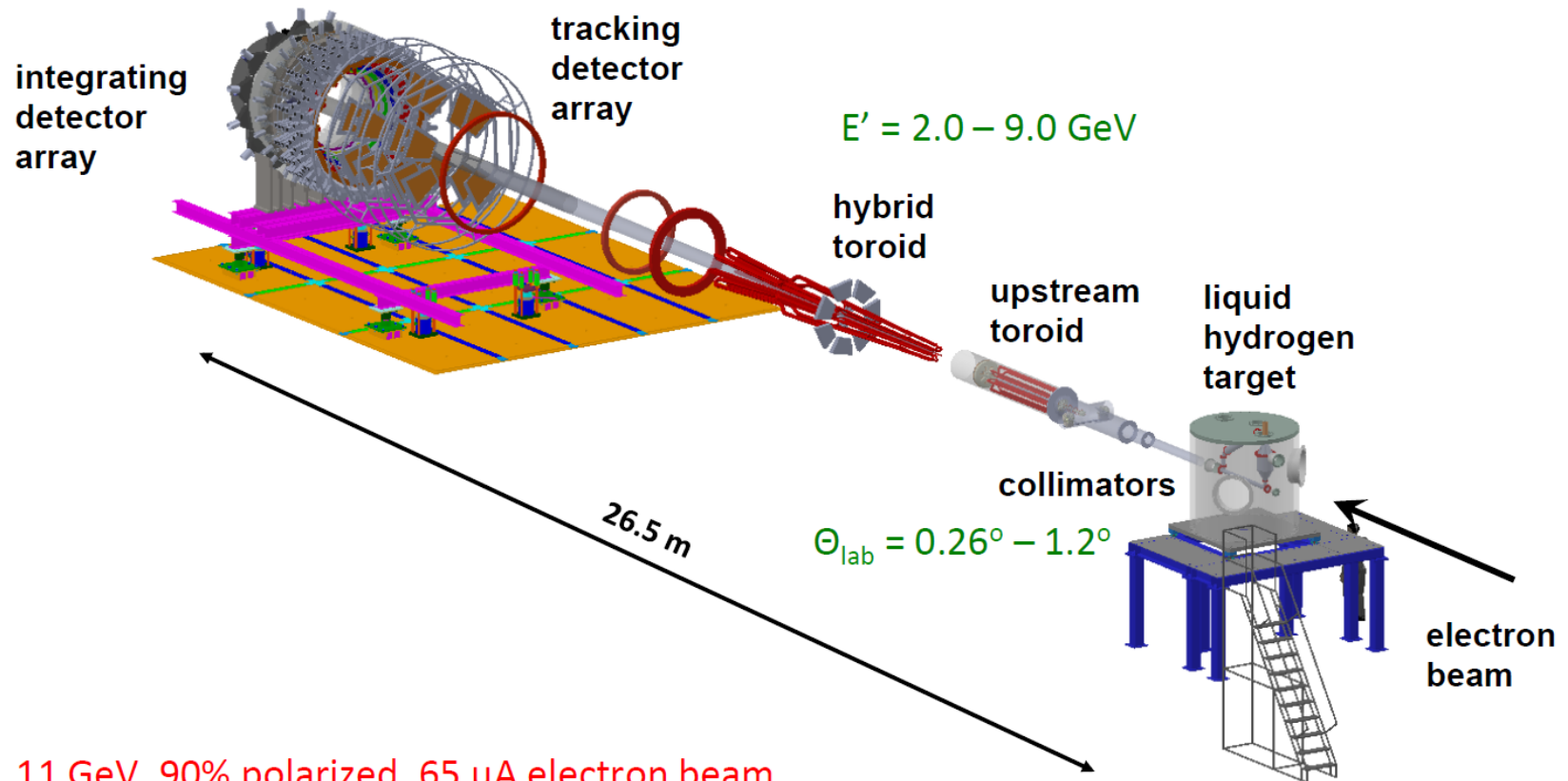
- Precision measurement of weak mixing angle via parity-violating Moller scattering
- DOE CD-0 approved, Dec. 2016
(project paused due to budget)
- Awaiting green light to proceed

SoLID

- Large acceptance, high luminosity
- Major experimental program of SIDIS and PVDIS emphasizing:
 - Standard model test
 - nucleon imaging

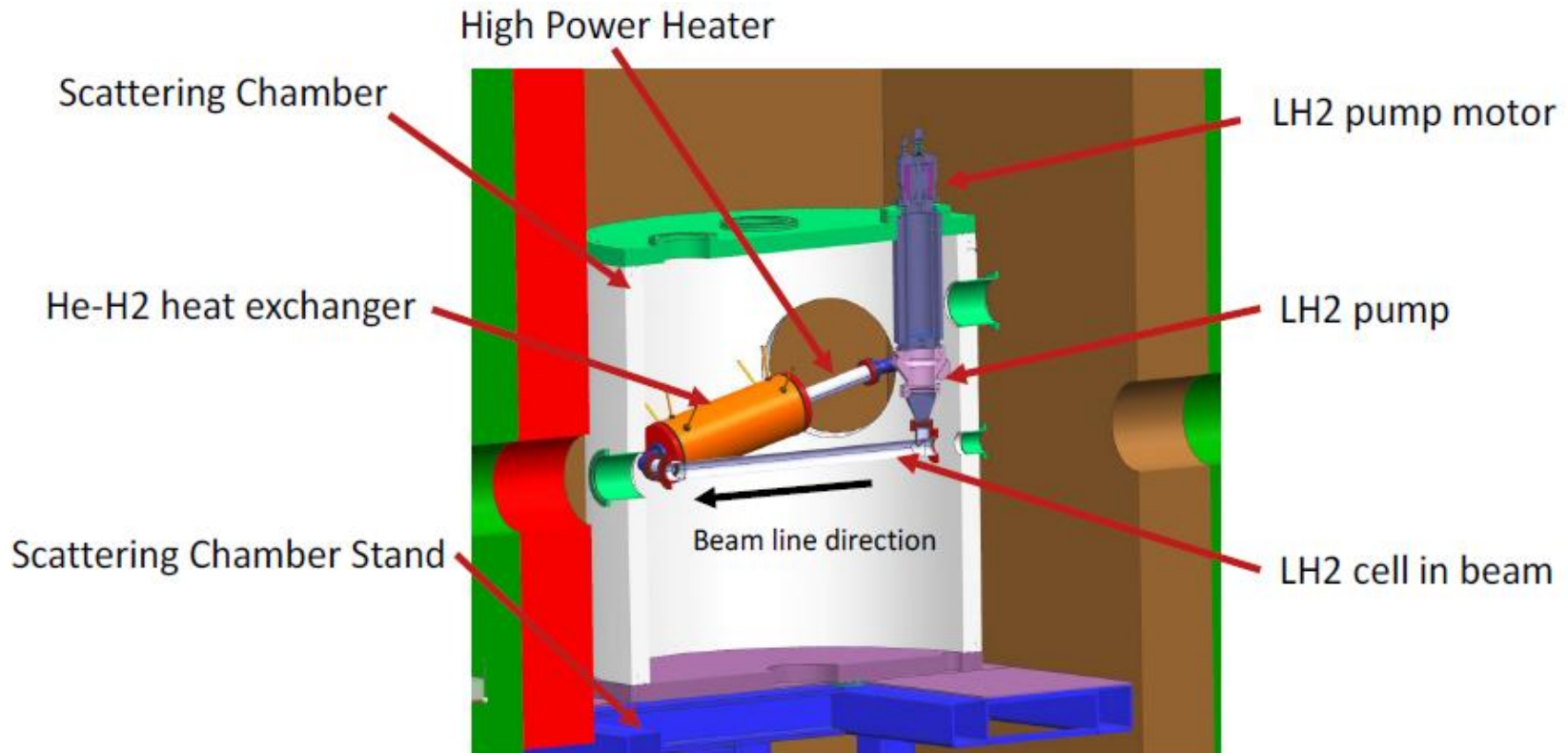


MOLLER Experiment: Conceptual Overview



- 11 GeV, 90% polarized, 65 μA electron beam
- 125 cm long, 4 kW LH_2 target
- Precision collimation (“2-bounce” design minimizes backgrounds)
- Novel two (warm) toroid spectrometer with 7 azimuthal segments; just fits into Hall A.
- Variety of integrating and counting detectors for main measurement and backgrounds

Moller target



EIC detector

- Some detectors with very high rates : Far Forward, Far Backward and Compton Polarimeter could use high rate capable, high radiation tolerant
- Talk by Whit on Thursday

Conclusion

- Superconducting detectors are a attractive for places where cryogenics is available
- They are very fast and have very good timing resolution (potentially picosecond level)
- Could operate close from cryogenic target
- Radiation tolerance and aging have to be studied but potentially much better than ionization detectors and semiconductors for metal superconductors
- Could allow to take advantage of full luminosity available at Jefferson Laboratory
- Still need a lot of R&D to allow photon counting and large scale detector, superconducting electronics needed too